The Plant Cell, Vol. 27: 3367–3382, December 2015, www.plantcell.org

Arabidopsis *Cell Division Cycle 20.1* Is Required for Normal Meiotic Spindle Assembly and Chromosome Segregation[OPEN]

Baixiao Niu,[a,1] Liudan Wang,[a,1] Liangsheng Zhang,[b] Ding Ren,[a] Ren Ren,[a] Gregory P. Copenhaver,[c,d] Hong Ma,[a,e,2] and Yingxiang Wang[a,2]

[a] State Key Laboratory of Genetic Engineering and Collaborative Innovation Center of Genetics and Development, Ministry of Education Key Laboratory of Biodiversity Sciences and Ecological Engineering, Institute of Plant Biology, School of Life Sciences, Fudan University, Shanghai 200438, China

[b] Center for Genomics and Biotechnology, Fujian Agriculture and Forestry University, Fuzhou 350002, China

[c] Department of Biology and the Carolina Center for Genome Sciences, University of North Carolina at Chapel Hill, Chapel Hill, North Carolina 27599-3280

[d] Lineberger Comprehensive Cancer Center, University of North Carolina School of Medicine, Chapel Hill, North Carolina 27599-3280

[e] Center for Evolutionary Biology, Institutes of Biomedical Sciences School of Life Sciences, Fudan University, Shanghai 200433, China

ORCID IDs: 0000-0003-1919-3677 (L.Z.); 0000-0002-7962-3862 (G.P.C.); 0000-0001-8717-4422 (H.M.); 0000-0001-6085-5615 (Y.W.)

Cell division requires proper spindle assembly; a surveillance pathway, the spindle assembly checkpoint (SAC), monitors whether the spindle is normal and correctly attached to kinetochores. The SAC proteins regulate mitotic chromosome segregation by affecting CDC20 (Cell Division Cycle 20) function. However, it is unclear whether CDC20 regulates meiotic spindle assembly and proper homolog segregation. Here, we show that the *Arabidopsis thaliana CDC20.1* gene is indispensable for meiosis and male fertility. We demonstrate that *cdc20.1* meiotic chromosomes align asynchronously and segregate unequally and the metaphase I spindle has aberrant morphology. Comparison of the distribution of meiotic stages at different time points between the wild type and *cdc20.1* reveals a delay of meiotic progression from diakinesis to anaphase I. Furthermore, *cdc20.1* meiocytes exhibit an abnormal distribution of a histone H3 phosphorylation mark mediated by the Aurora kinase, providing evidence that CDC20.1 regulates Aurora localization for meiotic chromosome segregation. Further evidence that CDC20.1 and Aurora are functionally related was provided by meiosis-specific knockdown of At-*Aurora1* expression, resulting in meiotic chromosome segregation defects similar to those of *cdc20.1*. Taken together, these results suggest a critical role for CDC20.1 in SAC-dependent meiotic chromosome segregation.

INTRODUCTION

Accurate chromosome segregation is required for genomic stability. In the mitotic cell cycle, following DNA replication, sister chromatids segregate to opposite poles. By contrast, meiosis involves two rounds of chromosome segregation: homologous chromosomes (homologs) separate during meiosis I and sister chromatids separate during meiosis II (Uhlmann, 2001). Several mechanisms ensure faithful chromosome segregation in both mitosis and meiosis. In particular, the spindle assembly checkpoint (SAC), a cell cycle surveillance pathway, delays chromosome segregation to allow correction of erroneous kinetochore attachments to the spindle or to allow unattached kinetochores to attach. SAC ensures proper chromosome alignment and the onset of anaphase, thereby facilitating faithful chromosome segregation (Homer et al., 2009; Musacchio and Ciliberto, 2012; Kim et al., 2013).

SAC components are highly conserved across eukaryotes, including the Ser/Thr kinases monopolar spindle 1 (MPS1), Aurora and Budding Uninhibited by Benomyl 1 (BUB1), and BUB3, and the non-kinase components Mitotic Arrest Deficient 1 (MAD1), MAD2, and BUB1 Related 1 (BUBR1) (Foley and Kapoor, 2013). The SAC proteins regulate chromosome segregation by sequestering CDC20 (Cell Division Cycle 20), preventing it from serving as a cofactor for the E3 ubiquitin ligase anaphase-promoting complex/cyclosome (APC/C) (Izawa and Pines, 2015). Correction of mistakes in kinetochore attachment to the spindle releases CDC20, which then activates APC/C for the removal of cohesin, thus promoting entry into anaphase (Salah and Nasmyth, 2000; Singh et al., 2014). In mitosis, the SAC proteins, including the protein kinase Aurora B, are recruited to unattached kinetochores to delay chromosome segregation until all chromosomes are correctly attached to the bipolar spindle (Kang and Yu, 2009; Zich and Hardwick, 2010). In animal cell lines and yeast, the centromeric localization of Aurora B depends on phosphorylation of Thr-3 on histone H3 (H3T3ph), which is mediated by Haspin (Dai et al., 2005; Kelly et al., 2010; Wang et al., 2010; F. Wang et al., 2012). Active

[1] These authors contributed equally to this work.

[2] Address correspondence to yx_wang@fudan.edu.cn or hongma@fudan.edu.cn.

The author responsible for distribution of materials integral to the findings presented in this article in accordance with the policy described in the Instructions for Authors (www.plantcell.org) is: Yingxiang Wang (yx_wang@fudan.edu.cn).

[OPEN]Articles can be viewed online without a subscription.

www.plantcell.org/cgi/doi/10.1105/tpc.15.00834

Aurora B then phosphorylates Ser-10 of histone H3 (H3S10ph), which affects chromosome condensation and segregation (Yamagishi et al., 2010; Castellano-Pozo et al., 2013). A recent study reported that a mutation in the *Arabidopsis thaliana Aurora1* gene results in a defect in meiotic chromosome segregation (Demidov et al., 2014), but the cellular defects of the aberrant meiosis were not described in detail.

The SAC components and their regulators have been studied extensively in both animal and fungal mitosis and meiosis (Mansfeld et al., 2011; Sun and Kim, 2012). By contrast, only a few SAC proteins have been found to be involved in plant meiosis, including the Arabidopsis MPS1 and Aurora kinases (Jiang et al., 2009; Demidov et al., 2014) and the rice (*Oryza sativa*) Bub1-Related Kinase (BRK1; M. Wang et al., 2012). CDC20 is a cofactor for both SAC and APC/C and has multiple roles in meiotic chromosome segregation in mice, *Drosophila melanogaster*, and bovine oocytes (Chu et al., 2001; Jin et al., 2010; Sun and Kim, 2012; Yang et al., 2014); however, the role of CDC20 in plant meiosis is unclear. Arabidopsis has five *CDC20*-like genes (*CDC20.1*-*CDC20.5*). *CDC20.1* and *CDC20.2* function redundantly in mitosis, while the three other genes appear to be pseudogenes (Kevei et al., 2011). Yeast two-hybrid assays demonstrated that Arabidopsis CDC20.1/2 could physically interact with the SAC protein MAD2/3, suggesting that association of CDC20 with SAC is conserved, at least in mitosis (Kevei et al., 2011).

Here, we show that *CDC20.1* is required for normal plant fertility and meiosis. Disruption of *CDC20.1* results in incomplete alignment of bivalents at metaphase I, leading to unequal chromosome segregation in both meiosis I and II. Cytological analysis shows that *cdc20.1* exhibits aberrant spindle morphology. In addition, histone modifications associated with cell cycle progression are altered in *cdc20.1*. H3S10ph is abnormally distributed, unlike its centromere-specific localization in normal meiocytes, and H3T3ph was greatly reduced. Finally, *cdc20.1* meiocytes exhibit delayed transition from metaphase I to anaphase I. These observations support a role for CDC20.1 in meiotic chromosome segregation by affecting SAC-dependent functions. Consistent with this model, meiosis-specific knockdown of the critical SAC factor *Aurora1* causes a meiotic chromosome segregation defect similar to that observed in *cdc20.1*, providing additional evidence that CDC20.1 plays a role in SAC-dependent meiotic chromosome segregation.

RESULTS

CDC20.1 Is Required for Male Fertility in Arabidopsis

CDC20.1 and *CDC20.2* have distinct expression patterns in somatic and reproductive tissues, whereas the three other genes lack detectable expression and are likely pseudogenes (Kevei et al., 2011). CDC20.1 and CDC20.2 share 99% protein sequence identity and have overlapping expression patterns in somatic tissues, suggesting functional redundancy of these proteins in the mitotic cell cycle. This idea is supported by the observations that simultaneous silencing of both genes results in a dwarf phenotype but that mutations in either gene alone do not cause developmental abnormalities (Kevei et al., 2011). In addition, *CDC20.1* is expressed at high levels in male meiocytes (Yang et al., 2011), but *CDC20.2* expression is nearly undetectable, suggesting that *CDC20.1* might have a more prominent role than *CDC20.2* in meiosis.

To investigate the function of *CDC20.1* in meiosis, we obtained two mutant alleles for *CDC20.1* from public T-DNA insertion line collections (Alonso et al., 2003). The T-DNA insertions are located in the fourth and the fifth exon, respectively (Supplemental Figure 1A). To distinguish these two alleles from the two previously identified weak alleles of *cdc20.1-1* and *cdc20.1-2* (Kevei et al., 2011), we named the two insertional alleles *cdc20.1-3* (CS369798) and *cdc20.1-4* (CS369975). We found that homozygous *cdc20.1-3* and *cdc20.1-4* plants showed no obvious defects in vegetative development nor in development of somatic anther tissues, as shown by semi-thin section microscopy (Figure 1A; Supplemental Figure 2A).

Mitotic chromosome morphologies showed no obvious differences between the wild type and *cdc20.1-3* (Supplemental Figure 2B), suggesting that mitosis in the mutant is normal. However, both mutant plants had greatly reduced fertility with obviously short siliques (Figure 1A), whereas heterozygous plants showed normal fertility, indicating that the mutations are recessive. Progeny of plants heterozygous for either mutant allele segregated mutant and normal phenotypes in a 1:3 ratio as expected for single Mendelian recessive mutations [*cdc20.1-3*, 44:141 for mutant/normal, $r^2_{(1:3)} = 0.145$, $P > 0.5$; *cdc20.1-4*, 43:136 mutant/normal, $r^2_{(1:3)} = 0.08$, $P > 0.5$]. Alexander staining for pollen viability showed a significant reduction in the number of viable pollen grains per anther ($P < 0.01$) in *cdc20.1-3* (43 ± 16/anther, $n = 24$) and *cdc20.1-4* (93 ± 32/anther, $n = 10$), in comparison to the wild type (508 ± 63/anther, $n = 14$) (Figure 1B). Pollen grains from both mutants had a range of sizes (Figure 1C; Supplemental Figure 2A), suggesting variable amounts of nuclear DNA, possibly due to meiotic defects. Consistent with this observation, unlike the four similarly sized wild-type microspores at the tetrad stage, both mutant anthers contained polyads with more than four microspores of variable sizes (Figure 1D). Furthermore, *cdc20.1-3*$^+$/*cdc20.1-4*$^+$ transheterozygous progeny created by crossing *cdc20.1-3*$^-$/*cdc20.1-3*$^+$ as the male parent with *cdc20.1-4*$^-$/*cdc20.1-4*$^-$ as the female parent showed similar defects in fertility (Figure 1). This cross produced a normal number of F1 seeds, and the subsequent progeny plants segregated in a 1:1 phenotypic ratio [mutant/normal = 18:16, $r^2_{(1:1)} = 0.12$, $P > 0.5$], indicating normal female development. Because the *cdc20.1-3* and *cdc20.1-4* alleles are independent T-DNA insertional mutants, these results strongly support the conclusion that the observed mutant phenotypes are caused by insertions in *CDC20.1*. However, the male sterility in both *cdc20.1-3* and *cdc20.1-4* is discordant with the normal fertility in *cdc20.1-1* and *cdc20.1-2* (Kevei et al., 2011), possibly because the T-DNA insertions in *cdc20.1-1* and *cdc20.1-2* are weak alleles.

To determine whether the T-DNA insertions in *CDC20.1* analyzed here disrupt its transcription, we used qRT-PCR to compare *CDC20.1* expression in the wild type and mutants and found no *CDC20.1* expression in *cdc20.1-3* and transcription upstream of, but not spanning, the T-DNA insertion in *cdc20.1-4* (Supplemental Figure 1C), indicating a truncated *CDC20.1* transcript. In addition, we performed RNAi-mediated *CDC20.1* knockdown driven by the meiosis-specific *DMC1* promoter, as used previously (Y. Wang et al., 2012). The results showed that the expression of *CDC20.1* was significantly decreased (*t* test, $P < 0.01$) in male meiocytes of

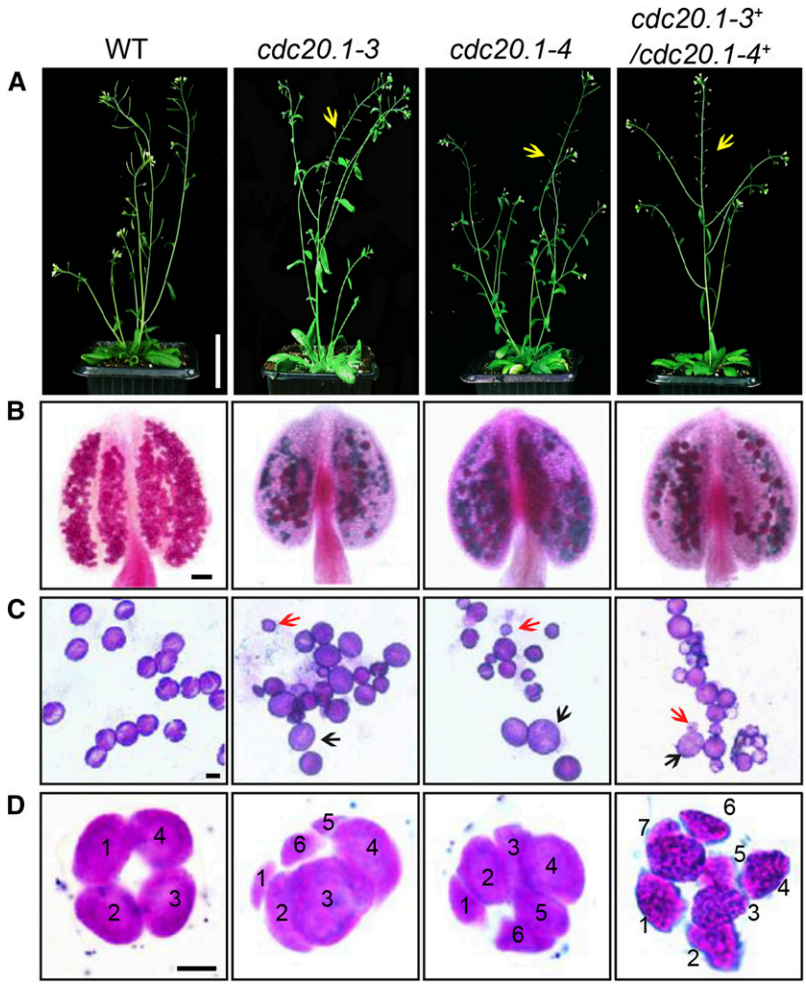

Figure 1. *CDC20.1* Mutant Plants Exhibit Reduced Fertility.

(A) Plant growth phenotypes of the wild type and mutants. Short siliques, indicating reduced fertility, are marked by arrowheads in *cdc20.1*. Bar = 5 cm.
(B) Pollen grain viability in wild-type and mutant anthers as assayed by Alexander Red staining. Anthers of the *CDC20.1* mutants show a significant proportion of dead pollen stained green and a few residual viable pollen grains. Bar = 50 μm.
(C) Wild-type pollen grains are of uniform size, while the size of *cdc20.1* pollen grains was variable, with larger (black arrows) and smaller (red arrows) grains than those of the wild type. Bar = 25 μm.
(D) Tetrad stage microspores in the wild type and mutants. Wild-type tetrad stage microspores have four equal size members, while *cdc20.1* samples at the same stage contain more than four microspores (numbered). Bar = 25 μm.

transgenic plants compared with the wild type, but not in inflorescences and leaves (Supplemental Figure 4B). Phenotypic analyses showed that the *ProDMC1*:*CDC20.1*^{RNAi} transgenic plants exhibited normal vegetative growth, but reduced fertility and meiotic defects (Supplemental Figures 4A and 4C), similar to the phenotypes of both *cdc20.1-3* and *cdc20.1-4*. These data strongly support the conclusion that *CDC20.1* is required for male fertility and meiosis in Arabidopsis.

CDC20.1 and *CDC20.2* Are Not Functionally Redundant in Meiosis

CDC20.1 and *CDC20.2* are redundant in mitotic cell division (Kevei et al., 2011), but their meiotic function has not been examined. To test for possible functional redundancy in meiosis, we obtained two mutant alleles for *CDC20.2* (At4g33260) with T-DNA insertions in the third intron (*cdc20.2-1*, Salk_114279c) and the fourth exon (*cdc20.2-2*, Salk_136710) (Supplemental Figure 1B), as described previously (Kevei et al., 2011). Consistent with previous observations, both homozygous *cdc20.2* mutants showed normal vegetative growth and reproductive development (Supplemental Figure 4A), suggesting *CDC20.2* is not essential for plant development.

Because the *CDC20.1* and *CDC20.2* loci are physically linked with only ~1 kb separating them, it is difficult to obtain the double mutant through crosses. Instead, we used meiosis-specific RNAi-mediated knockdown of either *CDC20.2* specifically (*ProDMC1*:*CDC20.2*^{RNAi}) or both genes simultaneously

using a target region conserved between the two genes (*ProDMC1*:*CDC20*^{RNAi}). As expected, *ProDMC1*:*CDC20.2*^{RNAi} plants had normal fertility, resembling the *cdc20.2* T-DNA insertional mutants (Supplemental Figure 4C). By contrast, *ProDMC1*:*CDC20*^{RNAi} plants showed defects in fertility and meiosis, similar to the *cdc20.1* single mutant (Supplemental Figures 4A and 4C), providing evidence that *CDC20.1* and *CDC20.2* are not redundant in meiosis.

CDC20.1 Is Required for Bivalent Alignment and Chromosome Segregation

The observation of polyads with more than four microspores in *cdc20.1* and *ProDMC1:CDC20.1*^{RNAi} plants suggests meiotic defects. Chromosome spreads stained with 4′,6-diamidino-2-phenylindole (DAPI) showed that *cdc20.1-3* and *cdc20.1-4* have normal chromosome morphology through diakinesis, similar to those in the wild type (Figure 2). At metaphase I, wild-type meiocytes have five well-aligned bivalents at the equatorial plane (Figure 2C), whereas 16.3% of *cdc20.1* cells (n = 98) showed abnormal alignment (Figures 2G, 2K, and 2O), leading to subsequent improper chromosome segregation at anaphase I (21%, n = 52) (Figures 2H, 2L, and 2P). At metaphase II, wild-type meiocytes have two sets of aligned chromosomes, and segregation results in four nuclei each containing five chromosomes (Figures 2Q to 2T). However, at a similar stage, 68.7% of *cdc20.1* cells (n = 64) had misaligned chromosomes (Figures 2V, 2Z, and 2D2), resulting in abnormal chromosome segregation (69.2%, n = 52) at anaphase II (Figures 2W, 2A2, and 2E2). As a consequence, *cdc20.1* meiocytes form more than four spores after meiosis (Figures 2X, 2B2, and 2F2), consistent with the observed polyads. Similar meiotic defects were also observed in *ProDMC1*:*CDC20.1*^{RNAi} and *ProDMC1*:*CDC20*^{RNAi} transgenic plants, but not in *ProDMC1*:*CDC20.2*^{RNAi} (Supplemental Figure 4C). These data demonstrate that *CDC20.1* is required for meiotic chromosome alignment and normal segregation.

In yeast, meiotic chromosome segregation requires the removal of cohesin in a two-step manner. Degradation of cohesin is controlled by the protease separase, which is activated by APC/C^{CDC20} through degradation of securin, a separase inhibitor (Peters, 2006). Arabidopsis SYN1 is a homolog of the yeast meiosis-specific cohesin REC8 (Meiotic recombination-deficient 8) (Cai et al., 2003). We examined SYN1 distribution in the wild type and *cdc20.1*. In wild-type pachytene meiocytes, SYN1 is distributed in a linear pattern along chromosomes (Figure 3A) and its signal decreases gradually after pachytene (Figures 3B and 3C). At anaphase I, SYN1 is only detected near the centromeric region (Figure 3D), consistent with previous observations (Chelysheva et al., 2010; Cromer et al., 2013), suggesting that the normal removal of cohesin from chromosome arms is required for homolog separation. At a similar stage, *cdc20.1* meiocytes displayed SYN1 patterns similar to those of the wild type (Figures 3A to 3D), supporting the idea that the observed defect in *cdc20.1* chromosome segregation is not caused by abnormal cohesin degradation. These results also suggest that the removal of cohesin on chromosome arms, to facilitate meiotic chromosome separation, is likely not mediated via CDC20.1-dependent APC/C activation in Arabidopsis.

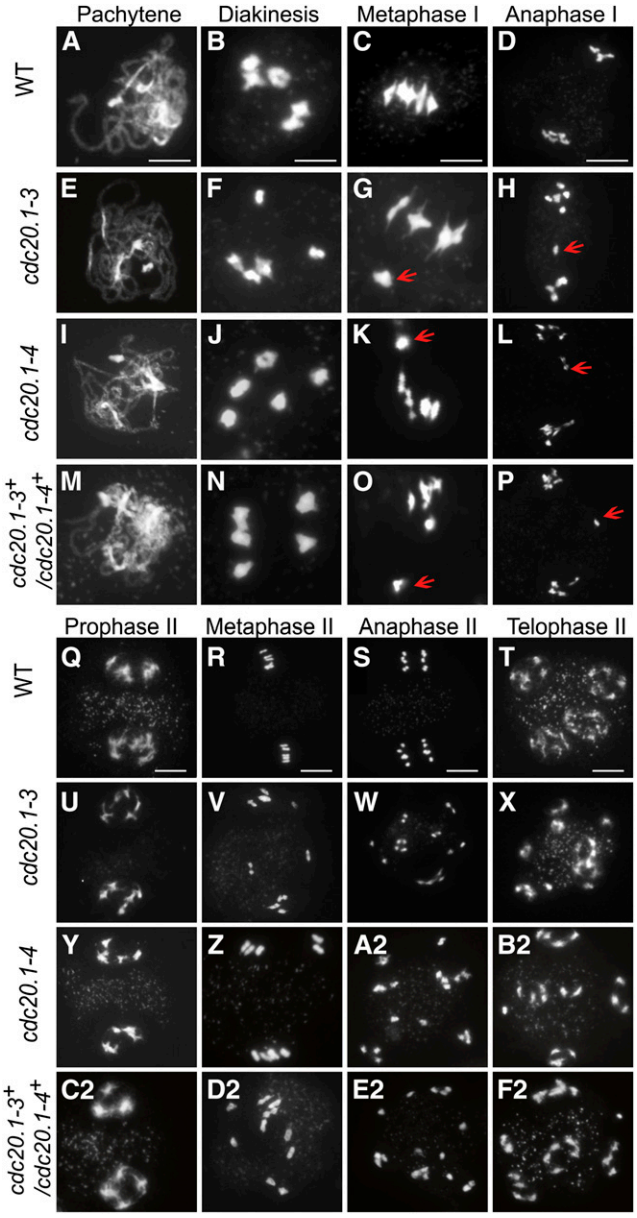

Figure 2. Aberrant Meiotic Phenotypes in *CDC20.1*-Deficient Meiocytes.

Meiotic chromosomes in wild-type and *cdc20.1* meiocytes: wild type (**[A]** to **[D]** and **[Q]** to **[T]**), *cdc20.1-3* (**[E]** to **[H]** and **[U]** to **[X]**), *cdc20.1-4* (**[I]** to **[L]** and **[Y]** to **[B2]**), and *cdc20.1-3*$^{+}$/*cdc20.1-4*$^{+}$ transheterozygous mutant (**[M]** to **[P]** and **[C2]** to **[F2]**). The misaligned chromosomes at metaphase I and lagging chromosomes at anaphase I in the mutants are indicated by arrows. Bars = 5 μm.

Kinetochore Biorientation of Bivalents Is Defective in *cdc20.1*

Misaligned metaphase I bivalents in *cdc20.1* suggest a defect in chromosome orientation between homologs. To test this hypothesis, we examined chromosomes using fluorescence in situ hybridization (FISH) using a probe for a 180-bp centromeric repeat (Y. Wang et al., 2012) and found that centromere signals showed

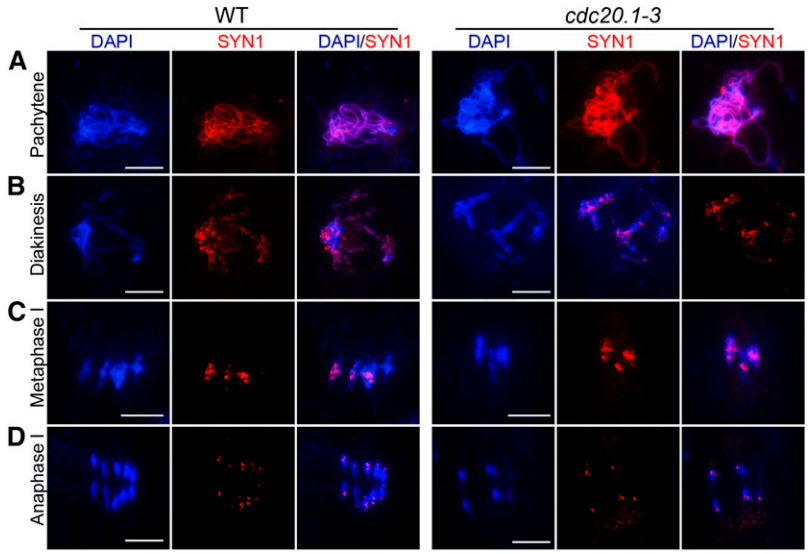

Figure 3. SYN1 Immunolocalization in *cdc20.1-3*.

Pachytene **(A)**, diakinesis **(B)**, metaphase I **(C)**, and anaphase I **(D)**. Left columns show chromosomes stained with DAPI (blue), the middle columns show SYN1 signals (red), and the right columns merge left columns with middle columns. Bars = 5 μm.

no obvious difference between the wild type and *cdc20.1-3* through pachytene (Figure 4A). At late diplotene and diakinesis, when the synaptonemal complex is disassembled, the wild-type homologous centromeres of a bivalent were detected as two signals (Figures 4B and 4C), whereas ~31.4% (n = 51) of the centromere signals in *cdc20.1-3* were associated with two independent bivalents (Figures 4B and 4C). At metaphase I, the five wild-type bivalents are aligned at the equatorial plate with sister chromatids orientated unidirectionally on the spindle, enabling segregation of homologous chromosomes to opposite poles (Figure 4D). In *cdc20.1-3*, 15.6% of cells (n = 32) had one bivalent failing to align properly with the other bivalents (Figure 4D, arrow), similar to the previously defined misorientation of kinetochores during meiosis I (Hauf and Watanabe, 2004). At anaphase I, unlike the five centromere signals observed on each side of the equatorial plate in the wild type, the mutant meiocytes exhibited abnormal chromosome segregation, consistent with the earlier misalignment (Figure 4E). At metaphase II, misaligned chromosomes were also observed in *cdc20.1-3* (Figure 4F, indicated by the arrow), supporting the idea that CDC20.1 is required for chromosome alignment in both meiosis I and II. At anaphase II, centromeric FISH signals segregated unevenly in *cdc20.1-3* (Figure 4G). We conclude that the misaligned chromosomes in *cdc20.1* are likely caused by disturbed kinetochore orientation between homologs and sister chromatids. This is supported by the observation of unequal distribution of CENP-A (also called HTR12), which is a kinetochore marker (Talbert et al., 2002; Kawabe et al., 2006) in *cdc20.1-3* (Supplemental Figure 3). Thus, these results support a role for CDC20.1 in kinetochore orientation during Arabidopsis meiosis.

CDC20.1 Is Required for Establishing Normal Spindle Morphology

Accurate chromosome segregation requires the establishment of proper spindle morphology and polarity (Watanabe, 2012). To investigate whether the abnormal chromosome alignment in *cdc20.1* is associated with aberrant spindle assembly, we examined spindle morphology by immunolocalization with an α-tubulin antibody. At prophase I, wild-type and *cdc20.1* meiocytes had similar perinuclear microtubule arrangements (Figure 5A). By metaphase I, the wild-type microtubules were organized into a typical bipolar structure (Figure 5A). A similar organization was observed surrounding the two clusters of chromosomes at metaphase II (Figure 5A). At telophase II, four nuclei are formed with microtubules between the nuclei. By contrast, at metaphase I, *cdc20.1* exhibited atypical spindle morphology, which could be caused by incorrect attachment of kinetochores to the spindles, as exemplified by lagging chromosomes (Figure 5A). Abnormal spindle morphology was also observed in *cdc20.1-3* at both metaphase II and telophase II (Figure 5A). Previous studies showed that poor alignment of chromosomes can cause longer spindles at metaphase I (Nagaoka et al., 2011; Kim et al., 2015). We also estimated the mean length and diameter of spindles in both the wild type and *cdc20.1-3* and found that *cdc20.1-3* had a significantly (t test, $P < 0.01$) longer average spindle length of 14.9 μm (n = 65) compared with the wild type length of 6.9 μm (n = 43) (Figure 5B). No significant difference (t test, $P > 0.05$) was found in the spindle diameter between the wild type and mutant (Figure 5B). These findings are consistent with previous findings that mutation in a rice SAC protein, BRK1, causes a longer average spindle length (M. Wang et al., 2012). Thus, we conclude that *CDC20.1* is required for proper spindle assembly and likely participates in SAC-dependent correction of erroneous attachments between microtubules and kinetochores during Arabidopsis meiosis.

Mutation in *CDC20.1* Delayed Metaphase I-Anaphase I Transition

In meiotic prophase I, kinetochores of sister chromatids should attach to microtubules from the same pole, whereas homologous

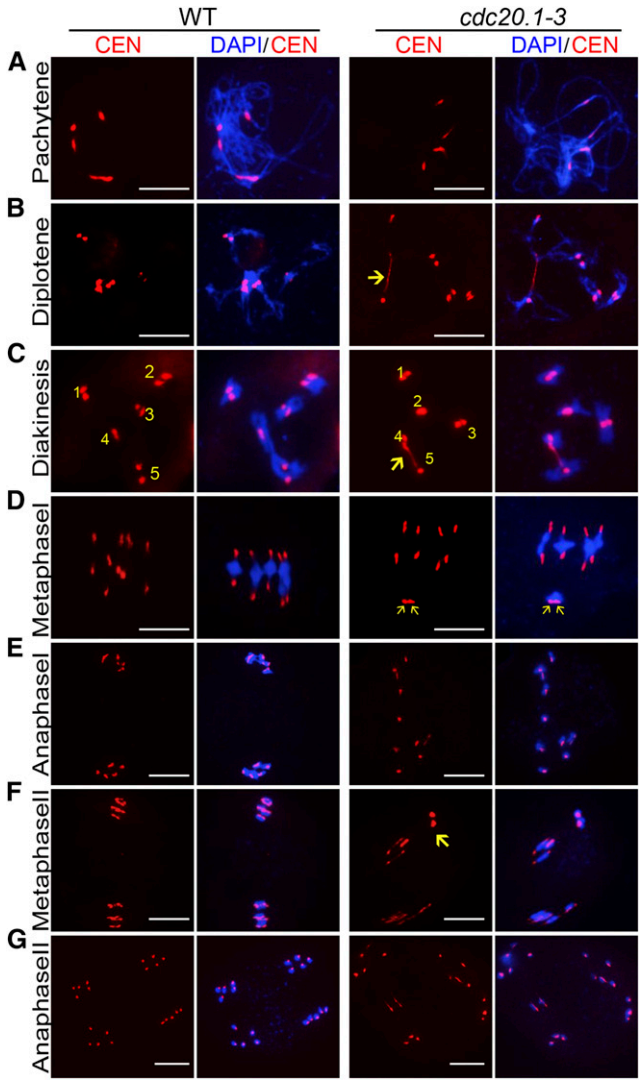

Figure 4. Chromosome Orientation Is Defective in *cdc20.1-3*.

Pachytene **(A)**, diplotene **(B)**, diakinesis **(C)**, metaphase I **(D)**, anaphase I **(E)**, metaphase II **(F)**, and anaphase II **(G)**. Chromosomes are stained with DAPI in blue, and centromeric regions are marked by red fluorescence. The wild type has five paired homologs (bivalent) at diakinesis and the paired centromeres in each bivalent are indicated with numbers **(C)**. The arrows indicate abnormal association at diplotene **(B)** and diakinesis **(C)**, and improper orientations at metaphase I **(D)** and metaphase II **(F)** in *cdc20.1-3*. Bars = 5 μm.

kinetochores should attach to microtubules from two different poles. Incorrect attachment triggers the SAC, which creates a "wait signal" until all kinetochores are properly attached to microtubules to prevent chromosome mis-segregation (Zamariola et al., 2014). Persistent incorrect attachment between spindles and kinetochores results in meiotic arrest at metaphase I in animals (Wassmann et al., 2003) and delayed meiotic progression in plants (Riehs et al., 2008; Cromer et al., 2012). Studies in multiple organisms estimate that meiotic prophase I occupies ~85% of the meiotic time course (Armstrong et al., 2003; Hamant et al., 2006). In Arabidopsis, meiocytes in an individual anther show a distribution of meiotic stages depending on the time of the day (Wang et al., 2004). To investigate whether CDC20.1 affects the timing of meiotic progress, we compared the distribution of meiocytes at different time points between the wild type and *cdc20.1-3* (Figure 6). Cell distribution through pachytene in both the wild type and mutant showed a similar pattern. Wild-type cells maintained a stable proportion of cells in diakinesis across six time points (Figure 6A), while the fraction of *cdc20.1* cells in diakinesis peaked at ZT2 (3 h after the start of the daily light cycle) and then decreased to a wild type level at ZT5 (Figure 6A), suggesting that *cdc20.1-3* cells are stalled at diakinesis, before transitioning to metaphase I, compared with the wild type. In addition, at similar time points, the *cdc20.1-3* had a persistently higher percentage of metaphase I cells compared with the wild type, except for at ZT1 (Figure 6B). Furthermore, the peak in the number of cells at anaphase I was delayed by 0.5 h in *cdc20.1-3* compared with the wild type (Figure 6C). Together, these results suggest that *cdc20.1-3* is defective in normal progression from metaphase I to anaphase I.

CDC20.1 Is Required for Centromere Localization of H3S10ph and Normal Levels of H3T3ph

Abnormal spindle assembly and metaphase I-anaphase I transition in *cdc20.1-3* suggest a defect in SAC function, as supported by the fact that yeast and animal CDC20 activates SAC (Sacristan and Kops, 2015). SAC is positively regulated by the Aurora kinase (Saurin et al., 2011), which is localized to centromeres at diakinesis. We hypothesized that the normal distribution of Aurora kinase might be affected in *cdc20.1*. Arabidopsis has three Aurora kinases, but no antibodies have been developed to examine their distribution. Nevertheless, Aurora phosphorylates Ser-10 of histone H3 (H3S10), which is highly conserved in animals, yeast, and plants, and its phosphorylated form serves as a marker for Aurora activity (Ditchfield et al., 2003; Kawabe et al., 2005; Gorbsky, 2015). We examined the distribution of H3S10ph in the wild type and *cdc20.1-3* by immunofluorescence with an H3S10ph antibody. In the wild type, H3S10ph was localized at centromeric regions at diakinesis (Figure 7A) and then along the whole chromosome at metaphase I (Figure 7B), which is in agreement with previous observations (Houben et al., 2007; Paula et al., 2013). By contrast, *cdc20.1-3* had a similar distribution of H3S10ph at metaphase I (Figure 7B), but at diakinesis it exhibited a diffuse distribution in contrast to the wild type (Figure 7A), suggesting that CDC20.1 is required for the centromere-specific Aurora localization at diakinesis.

It has been demonstrated that the centromeric localization of Aurora is directed by H3T3ph (Wang et al., 2010; Kurihara et al., 2011; F. Wang et al., 2012). We speculated that the abnormal distribution of H3S10ph in *cdc20.1-3* could be caused by defective H3T3 phosphorylation. Immunofluorescence analysis of both the wild type and *cdc20.1-3* with a H3T3ph antibody (Figure 8) showed that, at diakinesis, in wild-type meiocytes, H3T3ph is distributed along the chromosomes (Figure 8A), consistent with previous findings in both animals and plants (Manzanero et al., 2000; Caperta et al., 2008). By contrast, the H3T3ph signal was abolished in *cdc20.1-3* at a similar stage (Figure 8B). Together, our

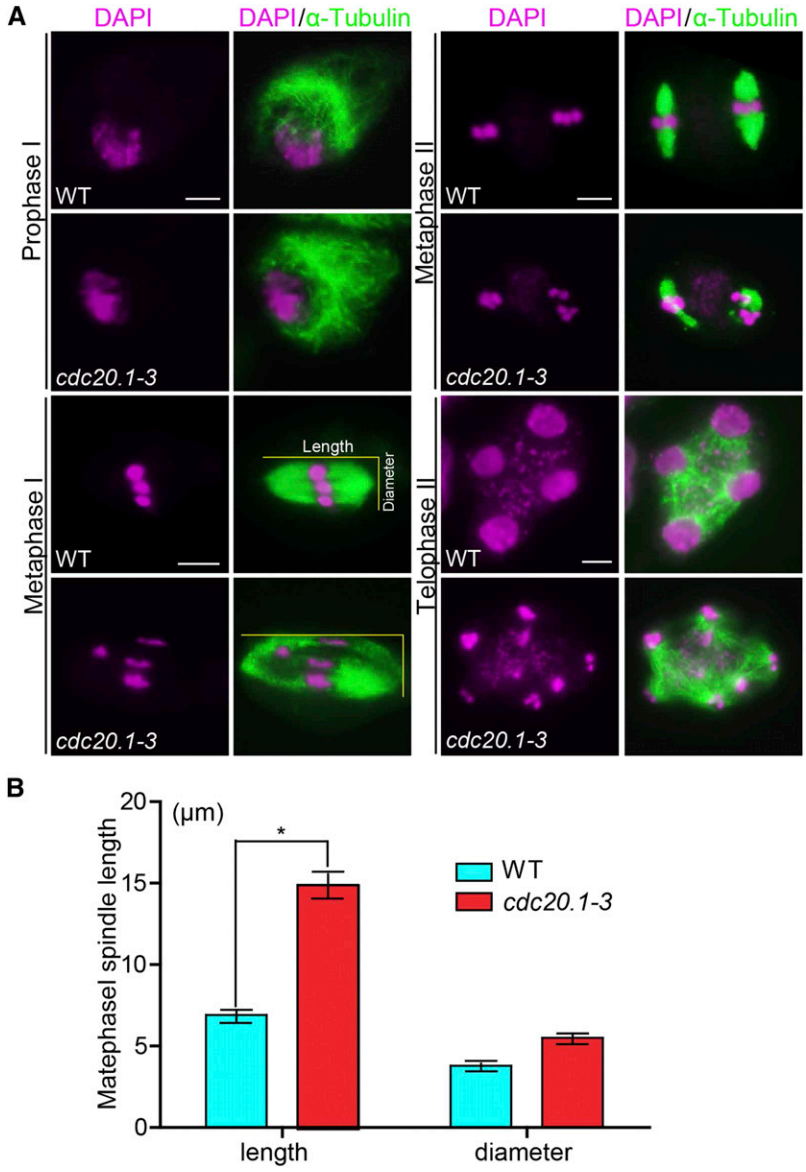

Figure 5. Spindle Morphology in Wild-Type and *cdc20.1-3* Meiocytes.

The spindle was detected by immunostaining with anti-α-tubulin antibody (green). Chromosomes were stained with DAPI (magenta).
(A) Comparison of spindle morphology at prophase I, metaphase I, metaphase II, and telophase II between the wild type and *cdc20.1-3*. Horizontal and vertical yellow lines refer the length and diameter of spindles, respectively. Bars = 5 μm.
(B) Quantification of the spindle length (illustrated in **[A]** with horizontal yellow bar) and the diameter of spindle equator (illustrated in **[A]** with vertical yellow bar) at metaphase I in the wild type (blue bars; $n = 43$) and *cdc20.1-3* (red bars; $n = 62$). Error bars represent SD; Student's *t* test was used for statistical analysis (*$P < 0.01$).

results suggest that CDC20.1 is required for faithful meiotic chromosome segregation likely by enabling H3T3 phosphorylation at diakinesis, thereby facilitating the centromere-specific distribution of Aurora and the resulting H3S10ph.

Meiosis-Specific Knockdown of *Aurora1* Causes a Chromosome Segregation Defect

Three Arabidopsis Aurora homologs are capable of phosphorylating H3S10 in vitro (Kawabe et al., 2005). Due to functional redundancy, single mutants have normal cell division, whereas the double mutants are either lethal or severely defective in mitosis (Van Damme et al., 2011; Demidov et al., 2014). A recent study provided evidence that the reduced expression of *Aurora* results in a defect in meiotic chromosome segregation (Demidov et al., 2014). However, the role of Aurora in Arabidopsis meiosis is still unclear. We generated *Aurora1* RNAi transgenic plants in which the transgenes were driven by the meiosis-specific *DMC1* promoter. qRT-PCR analysis showed the expression level of *Aurora1* was significantly reduced in *ProDMC1:Aurora1*^{RNAi} transgenic

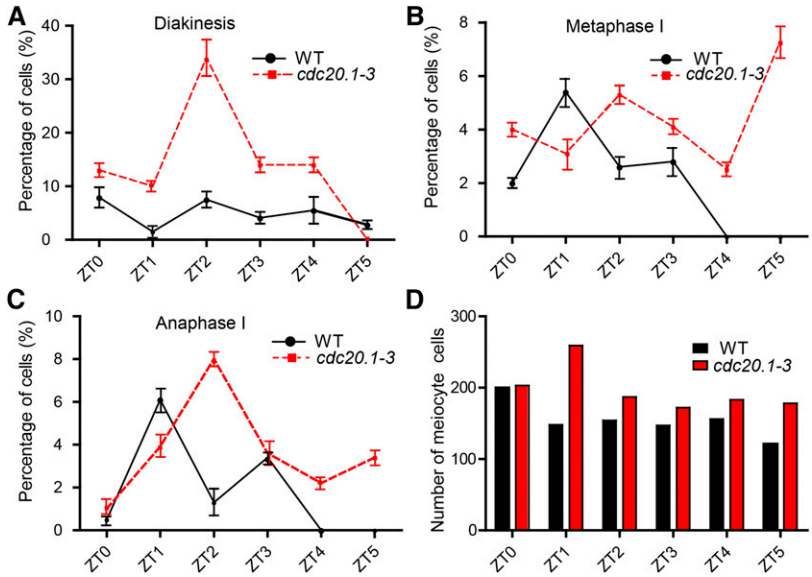

Figure 6. Stage-Dependent Meiocyte Distribution at Different Time Points in the Wild Type and *cdc20.1-3*.

The *y* axes represent the percentage of cells in diakinesis, metaphase I, and anaphase I at each time point, while the *x* axes represent the time points after starting the daily light cycle. We defined ZT0-ZT5 as 2 to 4.5 h with 0.5-h intervals. Error bars represent SD.

(A) The percentage of diakinesis meiocytes in *cdc20.1-3* is higher than that in the wild type, especially at ZT2.

(B) Metaphase I meiocytes persist in *cdc20.1-3* compared with the wild type after ZT2.

(C) The peak of anaphase I cells in *cdc20.1-3* is delayed by 0.5 h in comparison to the wild type.

(D) Total number of meiocytes counted at each time point.

male meiocytes compared with the wild type ($P < 0.01$) (Figure 9A). The *ProDMC1:Aurora1*^{RNAi} transgenic plants showed normal vegetative growth, but greatly reduced fertility, as shown by short siliques (Figure 9B) and a large number of dead pollen grains (Figure 9C). Analysis of chromosome morphology by FISH with a centromere probe showed that chromosome morphology and centromere signals had no obvious differences between wild-type and *ProDMC1:Aurora1*^{RNAi} transgenic plants through diakinesis (Figure 9D). At metaphase I, the wild type had five bivalents aligned at the equatorial plate, while *ProDMC1:Aurora1*^{RNAi} chromosomes aligned asynchronously at the equatorial plate (Figure 9D) and segregated unequally at anaphase I and anaphase II (Figure 9D), similar to the *cdc20.1* single mutant phenotypes. Given that Aurora is a critical component of SAC, the similar defects of the *cdc20.1* mutant and Aurora knockdown plants support a role of CDC20.1 in regulating SAC-dependent meiotic chromosome segregation.

DISCUSSION

Functional Diversification of Recently Tandem Duplicated *CDC20* in Plant Meiosis

CDC20 is highly conserved in eukaryotes (Smith et al., 1999). Unlike animals with a single *CDC20* locus, Arabidopsis has five *CDC20* homologs. *CDC20.1* and *CDC20.2* are functionally redundant in mitosis (Kevei et al., 2011), whereas the other three genes are probably pseudogenes. Previous studies showed that *CDC20.1* is expressed in vegetative and reproductive tissues, while *CDC20.2* is restricted in vegetative tissues (Kevei et al., 2011), indicative of functional diversification.

Here, we investigated the function of *CDC20.1* and *CDC20.2* in meiosis and found that only *CDC20.1* is indispensable for male meiosis. To test for functional redundancy, we used an RNAi-mediated knockdown strategy to simultaneously reduce *CDC20.1* and *CDC20.2* expression in transgenic plants and observed a meiotic phenotype similar to *cdc20.1* single mutants (Supplemental Figure 4). By comparison, meiosis-specific knockdown of *CDC20.2* alone did not affect fertility or meiosis (Supplemental Figure 4). Moreover, analyses of *CDC20.1* and *CDC20.2* expression in reciprocal mutant backgrounds found that *CDC20.1* expression in the *cdc20.2* mutant showed a 5- to 10-fold increase compared with the wild type, whereas *CDC20.2* expression was the same in *cdc20.1* as in the wild type (Supplemental Figures 1D and 1E). These results suggest that elevated *CDC20.1* expression may compensate for loss of *CDC20.2* function.

CDC20.1 and *CDC20.2* are present on chromosome 4 as tandem duplicates within a 6-kb region separated by a 1-kb intergenic region. The region containing *CDC20.1* and *CDC20.2* is syntenic in *A. thaliana*, *Arabidopsis lyrata*, and *Capsella rubella*, but not in *Brassica rapa* and *Eutrema salsugineum* (Figure 10A), implying that the duplication was recent, after the divergence of lineage I and lineage II ~27 to 33 million years ago (MYA) in Brassicaceae, but before the separation of the *Arabidopsis* and *Capsella* genera (Figure 10B), which occurred ~9.12 MYA (Kagale et al., 2014) or earlier ~15 to 17 MYA (Huang et al., 2015). This period was accompanied by the diversification of taxa in lineage I in Brassicaceae. The ratio of nonsynonymous-to-synonymous

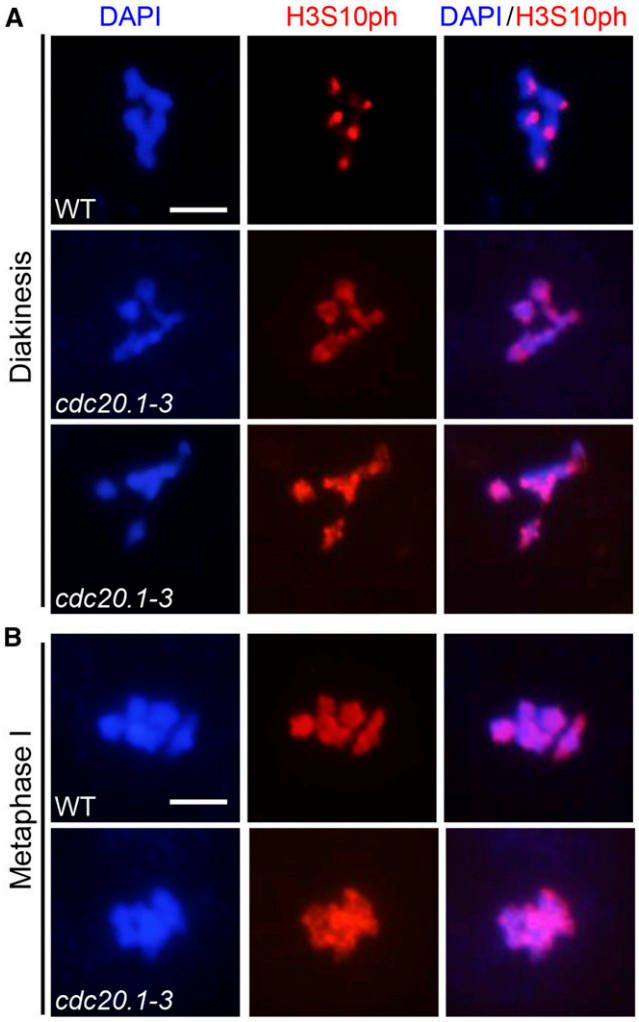

Figure 7. CDC20.1 Is Required for the Recruitment of Centromeric H3S10ph.

Distribution of H3S10ph in the wild type and *cdc20.1-3* in diakinesis **(A)** and metaphase I **(B)**. Left column shows chromosomes stained with DAPI (blue), the middle column shows H3S10ph signals (red), and the right column shows the merged image. Bars = 5 μm.

nucleotide changes (ω = dN/dS) is used widely to infer the effect of natural selection on protein-coding genes. The value for Arabidopsis *CDC20.1* and *CDC20.2*, ω = 0.0838 (dS = 0.0858, dN = 0.0072), is very low, reflecting strong purifying selection and highly conserved function. Considering these results, the subfunctionalization of *CDC20.1* and *CDC20.2* likely results from their differential temporal and spatial expression patterns, which may be mediated by distinct *cis*-regulatory elements, but this remains to be tested experimentally.

A Potential Role of CDC20.1 in Meiotic Chromosome Segregation

The faithful segregation of genetic material into daughter cells during cell division is crucial for the production of healthy progeny (Jin et al., 2010; Whitfield et al., 2013; Teixeira et al., 2014). Chromosome segregation is regulated by several mechanisms, including cohesion degradation and SAC-dependent surveillance (Musacchio and Ciliberto, 2012). The stepwise removal of cohesin during meiosis is well studied in human, mouse, and plants (Salah and Nasmyth, 2000; Riedel et al., 2006; Cromer et al., 2013). Cohesin is protected by SGO proteins in the centromere region during meiosis I and is released by separase in a process that is conserved among eukaryotes (Zamariola et al., 2013). In *Xenopus laevis*, Drosophila, and yeast, the activation of separase requires degradation of securin mediated by the APC/C^{CDC20}-dependent pathway (Salah and Nasmyth, 2000; Terret et al., 2003; Kudo et al., 2006; Swan and Schüpbach, 2007). However, *cdc20.1* has five normal bivalents (Figure 2) and a normal distribution of meiosis-specific cohesin SYN1 through anaphase I (Figure 3), supporting the idea that its meiotic chromosome segregation defects are not caused by inappropriate cohesin degradation. It is also possible that SYN1 is not the sole substrate targeted by APC/C^{CDC20}, at least in Arabidopsis meiosis. Another possibility is that CDC20 is functionally redundant with other APC/C activators.

Arabidopsis CDC20.1 can physically interact with SAC components Mad2 and BubR1 (Kevei et al., 2011), leading to the hypothesis that CDC20.1 is involved in SAC function; however, this hypothesis has not yet been tested in plants. Here, we

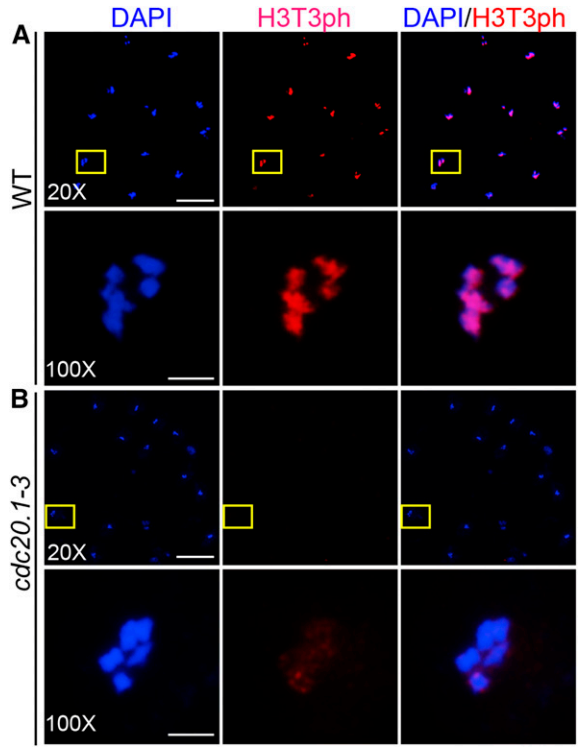

Figure 8. CDC20.1 Is Required for H3T3 Phosphorylation in Meiocytes.

Immunolocalization of H3T3ph (red) at diakinesis of the wild type **(A)** and *cdc20.1-3* **(B)**, with chromosomes visualized by DAPI staining (blue). The boxed regions in **(A)** indicate a meiotic cell, which was shown under a 100× microscope in **(B)**. 20× (bars = 20 μm) and 100× (bars = 5 μm) indicate microscope magnification.

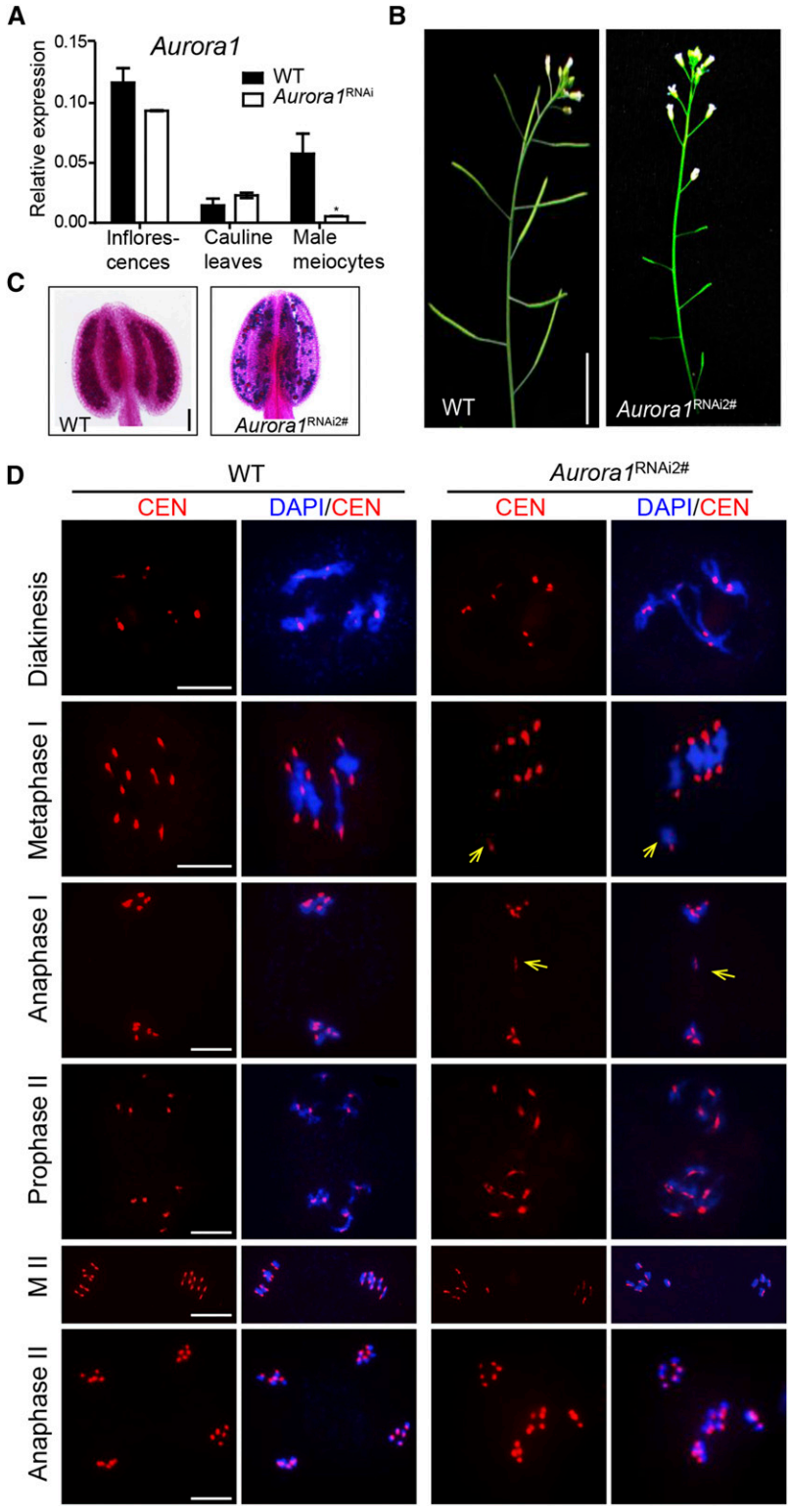

Figure 9. Phenotypic Analysis of *ProDMC1*:*Aurora1*^{RNAi} Plants.

(A) Analysis of expression level of *Aurora1* in different tissues of *ProDMC1*:*Aurora1*^{RNAi} transgenic plants (*Aurora1*^{RNAi}) and the wild type (*$P < 0.01$, Student's *t* test).

(B) The short siliques of *ProDMC1*: *Aurora1*^{RNAi} plants compared with the wild type indicate reduced fertility. Bars = 5 cm.

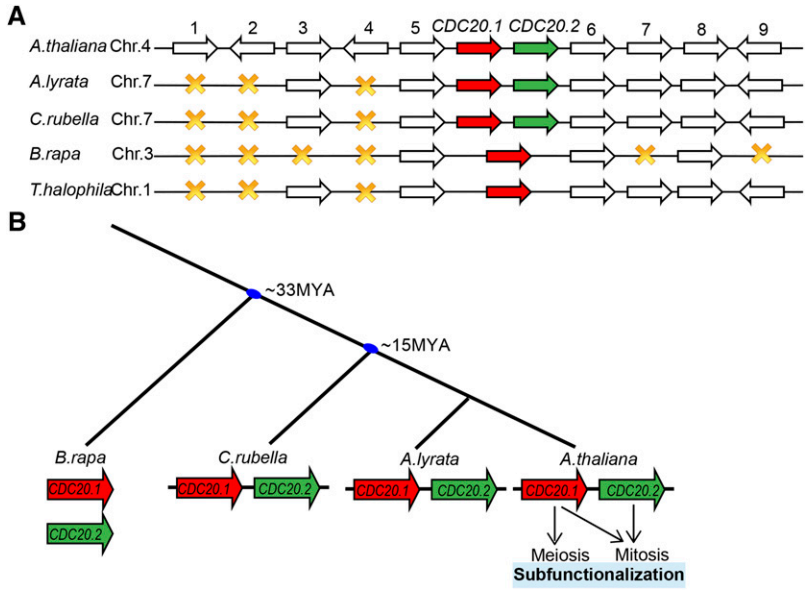

Figure 10. Analysis of *CDC20.1* and *CDC20.2* in Related Species.

(A) Conserved tandem arrangements of *CDC20.1* and *CDC20.2* in *A. thaliana*, *A. lyrata*, and *C. rubella*. Genes that exhibit conserved synteny in the different species are shown as arrows (red, *CDC20.1*; green, *CDC20.2*; white, flanking genes), while yellow crosses indicate missing genes at the corresponding positions. Species names and chromosome numbers are shown to the left.

(B) A model proposing the origin of *CDC20.1* and *CDC20.2* as tandem duplicates in *A. thaliana*, *A. lyrata*, and *C. rubella.* The estimated separation time of *A. thaliana* and *C. rubella* is ~15 to 17 MYA, while the estimated separation time of lineage I and II is ~27 to 33 MYA in Brassicaceae (Huang et al., 2015). The blue ovals at the nodes indicate the estimated separation time.

provided several lines of evidence to support the role of CDC20.1 in meiotic chromosome segregation through a SAC-dependent process. First, *cdc20.1* is defective in bivalent alignment at metaphase I (Figure 2), suggesting a possible defect in spindle checkpoint control. This agrees with a previous report that proper chromosome alignment requires establishment of spindle attachment and correct biorientation by SAC associated with CDC20 (Musacchio and Ciliberto, 2012). Second, unequal chromosome segregation at anaphase I indicates defective spindle structure or function. This is supported by the abnormal spindle morphology (Figure 5) observed in *cdc20.1*. Third, the distribution of various stages of meiotic cells at different time points demonstrated that the kinetics of diakinesis and metaphase I in *cdc20.1* cells differ from those in the wild type, similar to the finding that animal cells are arrested at metaphase I in the absence of SAC proteins (Wassmann et al., 2003). Fourth, patterns of H3S10 and H3T3 phosphorylation were altered in *cdc20.1* compared with the wild type (Figures 7 and 8), providing additional indirect evidence for the involvement of CDC20.1 in SAC. Histone H3S10 is one of the substrates of the SAC activator Aurora (Kawabe et al., 2005), whose localization at the centromere requires histone H3T3ph (Wang et al., 2010; F. Wang et al., 2012). Finally, meiosis-specific knockdown of *Aurora1* phenocopied the defects in meiotic chromosome alignment and segregation observed in *cdc20.1* (Figure 9), similar to previous studies in yeast and animals (Ditchfield et al., 2003; Morrow et al., 2005), further supporting a potential role of CDC20.1 in the regulation of SAC during Arabidopsis meiosis.

On the basis of these results, we present a model to illustrate the mechanism of CDC20.1 function in meiotic chromosome segregation (Figure 11). In the wild type, between diakinesis and metaphase I, kinetochores on each bivalent are attached to spindle microtubules. When erroneous attachments occur, they can be corrected following their detection by SAC. CDC20.1 promotes H3T3 phosphorylation, which facilitates the localization of the SAC activator Aurora at the centromere, thereby promoting phosphorylation of H3S10 to ensure the proper chromosome alignment at metaphase I and subsequent segregation at anaphase I (Figure 11, left panel). In the absence of CDC20.1, lack of H3T3ph results in nonspecific H3S10ph distribution, thus affecting SAC function. As a consequence, erroneous spindle attachments can persist and cause chromosome misalignment at

Figure 9. (continued).

(C) Pollen grain viability in wild-type and transgenic anthers as assayed by Alexander staining. Bars = 50 μm.

(D) Chromosome morphology in *ProDMC1:Aurora1*^{RNAi} meiocytes with misalignment of homologs at metaphase I (yellow arrows) and unequal chromosome segregation at anaphase I (yellow arrow marks lagging DNA) and meiosis II. Bars = 5 μm.

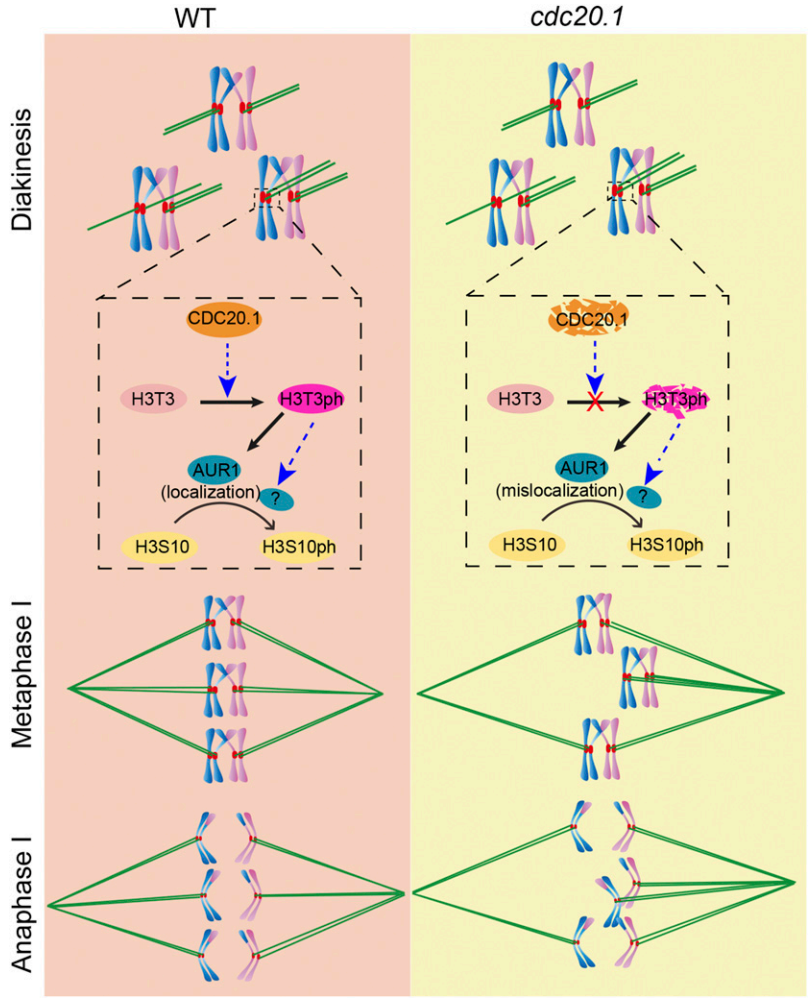

Figure 11. A Model for CDC20.1 Function in SAC-Dependent Meiotic Chromosome Segregation.

In the wild type, between diakinesis and metaphase I, kinetochores (red circles) on each bivalent are attached to spindle microtubules (green bars). Erroneous attachments (highlighted in the dashed box) need to be corrected following their detection by SAC. CDC20.1 promotes H3T3 phosphorylation, which facilitates the localization of the SAC activator Aurora at the centromere, thereby promoting phosphorylation of H3S10 to ensure the proper chromosome alignment at metaphase I and subsequent segregation at anaphase I (left panel). In the absence of CDC20.1, lack of H3T3ph results in nonspecific H3S10ph distribution, thus affecting SAC function. As a consequence, erroneous spindle attachments can persist and cause chromosome misalignment at metaphase I and unequal segregation at anaphase I (right panel). Dashed blue arrows indicate indirect interaction, and the question marks indicate unknown factors, which may be involved in the same step as AUR1. Pink ovals indicate H3T3 protein, magenta ovals indicate the phosphorylated H3T3, and blue ovals indicate AUR1 protein. The solid filled ovals refer normal proteins, while the patchy ovals indicate proteins with loss of function.

metaphase I and unequal segregation at anaphase I (Figure 11, right panel).

Conservation and Diversification of CDC20 in Cell Division between Animals and Plants

CDC20 was first shown to be required for the activation of APC/C to initiate the mitotic metaphase-anaphase transition in *Saccharomyces cerevisiae* (Hartwell et al., 1973). Further studies demonstrated that MAD2 interacts with CDC20 and inhibits its activation of APC/C in yeast and animals (Fang et al., 1998; Sudakin et al., 2001). Recently, Arabidopsis CDC20 was shown to interact with mitotic cyclins CYCA1;1 and CYCB2;2, and SAC proteins such as MAD2 and BubR1 (Kevei et al., 2011), indicating a conserved function for CDC20 in substrate degradation and SAC. However, unlike other organisms, plants have multiple CDC20 copies, opening the possibility that they have functionally diverged.

Recently, several *CDC20*-like genes have been found to regulate meiosis-specific APC/C activity or be otherwise involved in fertility (Pesin and Orr-Weaver, 2008; Cooper and Strich, 2011). For example, the yeast *CDC20*-like gene *Ama1* is required for metaphase I spindle assembly and cohesion degradation (Cooper et al., 2000; Oelschlaegel et al., 2005; Tan et al., 2011). Also, in Drosophila, a distant member of *CDC20*, *cort*, is expressed specifically during oogenesis and regulates the metaphase I-to-anaphase I transition (Page and Orr-Weaver, 1996; Harms et al.,

2000; Chu et al., 2001). In addition, CDC20 is also required for fertility and meiosis I in female mice (Jin et al., 2010). However, the function of CDC20 in plant meiosis was previously unknown. Additional information for CDC20's role in plant meiosis comes from studies of two Arabidopsis meiotic cell division factors OSD1 and PANS1, which can physically interact with CDC20 in yeast two-hybrid assays (Cromer et al., 2012, 2013). These observations indicate a possible role for CDC20 in the degradation of cyclin and cohesin during chromosome segregation, but this hypothesis has yet to be experimentally tested. A more recent study showed that defective CDC20 in bovine oocytes results in abnormal spindle morphology and reduced *MAD2* expression (Yang et al., 2014), but the underlying mechanism is still unclear. Here, we demonstrated that plant CDC20 is required for meiotic chromosome segregation, probably by regulating SAC function, in contrast to animal or yeast homologs, which are involved in APC/C activation. Given that accurate chromosome segregation is important for genome stability and human fertility, the identification of CDC20 as a regulator of SAC-dependent chromosome segregation could have significant implications for human reproductive health and crop genetic breeding.

METHODS

Plant Material and Growth Conditions

In this study, *Arabidopsis thaliana*, ecotype Col-0 plants were used as the wild type. Two Arabidopsis *CDC20.1* T-DNA insertional lines, *cdc20.1-3* (CS369798) and *cdc20.1-4* (CS369975), and two *CDC20.2* T-DNA insertional lines, *cdc20.2-1* (SALK_114279c) and *cdc20.2-2* (SALK_136710), were used. All mutants were obtained from the ABRC. Arabidopsis plants were grown in an automatically controlled greenhouse under a 16-h-day/8-h-night photoperiod, at 20°C with 70% humidity. For in vitro culture, sterilized Arabidopsis seeds were plated on medium containing 0.5× nutrient solution supplemented with 0.5% (w/v) sucrose and 1% (w/v) agar. The two-week-old plants were transferred to a growth chamber with a 16-h-day/8-h-night photoperiod, at 20°C with 70% humidity.

Morphological Analysis of Plants

Plants were photographed with a Canon digital camera (Canon500D). Pollen viability was analyzed by staining with Alexander staining (Peterson et al., 2010) at 37°C for 2 h. Tetrad dissection and pollen morphology were assayed as described previously (Wang et al., 2014). Images were collected with a Zeiss Axio Imager A2 microscope. Transverse sections of plastic-embedded anthers were obtained using the Historesin kit following the manufacturer's instructions (Leica). Then, 2-μm-thick sections were stained with 0.25% toluidine blue.

Expression Analysis

Total RNA was extracted from stage 4-7 inflorescences and leaves using Trizol reagent (Invitrogen) according to the manufacturer's instructions. Male meiocytes were obtained as previously described (Yang et al., 2011). First-strand cDNA was synthesized using the First Strand cDNA Synthesis kit (Promega). Reverse transcription products were then used as the template for PCR reactions. Quantitative RT-PCR analyses were performed using the Step One Plus Real-Time PCR system (Applied Biosystems). Reactions contained the SYBR Green QPCR Master Mix (TaKaRa) in a final volume of 25 μL with the appropriate primers (Supplemental Table 1). PCR conditions were 95°C for 5 min followed by 40 cycles of 95°C for 15 s, 55°C for 15 s, and 72°C for 15 s. Each experiment included three independent biological replicates. Samples were normalized using At-*EF1α* expression. Relative expression levels were measured using the $2^{\Delta Ct}$ analysis method. RT-PCR primers are listed in Supplemental Table 1.

Cytological Procedures

Chromosome spreads, FISH, and immunostaining were performed as described previously (Wang et al., 2014). The Histone H3 phosphorylation was detected using rabbit antiserum specifically recognizing the histone H3 Ser-10 phosphorylation peptide (Millipore), diluted 1:400, and rabbit antiserum recognizing the histone H3T3 phospho-peptide (Millipore), diluted 1:800. SYN1 immunolocalization was performed as described previously (Chelysheva et al., 2010), and rabbit anti-SYN1 was used at a 1:200 dilution. The slides were observed using a Zeiss Axio Imager A2 fluorescence microscope.

Immunolocalization of Tubulin

Inflorescences were fixed in methanol:acetone (4:1). The appropriately staged buds were digested for 2 h at 37°C as described previously (Wang et al., 2014). Meiocytes were stripped, squashed, and immobilized on poly-L-Lys-coated slides and air-dried for subsequent analysis. Slides were incubated in PBS with 1% Triton X-100 for 1 h at room temperature. After two rinses with PBS with 0.1% Tween 20, slides were incubated overnight at 4°C in primary antibodies of mouse antitubulin (Beyotime AT819) at a 1:200 dilution in PBS with 1% BSA and then washed three times in PBS with 0.1% Tween 20 for 10 min each. After 2 h of incubation at 37°C with the secondary antibodies in PBS with 1% BSA, slides were washed in PBS with 0.1% Tween 20 three times for 10 min each and then stained with 8 μL DAPI (Vector Laboratories) and observed with a Zeiss Axio Imager A2 fluorescence microscope.

Statistical Analysis of Meiocyte Distribution at Different Stages

Wild-type and CDC20.1 mutant plants were grown under the same conditions (as described above) until after bolting. Six time points after exposure to light (Huang et al., 2015) were defined (i.e., 2 h [ZT0], 2.5 h [ZT1], 3 h [ZT2], 3.5 h [ZT3], 4 h [ZT4], and 4.5 h [ZT5]), and wild-type and mutant inflorescences were collected at each time point. Inflorescences were fixed in Carnoy's fluid with ethanol:acetic acid (3:1). Chromosome behavior was analyzed using chromosome spreads stained with DAPI. The meiocytes were observed and counted under a fluorescence microscope (Zeiss Axio Imager A2), and the data were analyzed using Prism 5.0 software.

Plasmid Construction and Plant Transformation

For RNAi plasmid construction, a specific ~400-bp region of each gene for amplification using primers (Supplemental Table 1) that included restriction sites *Nco*I/*Spe*I and *Xba*I/*Sal*I, respectively. The sense and antisense fragment were digested with *Nco*I-*Spe*I and *Sal*I-*Xba*I, respectively, and sequentially cloned into the same sites in the pMeio*DMC1*-Intron vector. The constructs were introduced into *Agrobacterium tumefaciens* GV3101 for wild-type Arabidopsis transformation using the floral-dip method (Clough and Bent, 1998). Positive T1 plants were screened on 0.5× Murashige and Skoog medium containing 25 mg/L hygromycin and transferred to soil in a greenhouse under 20°C, 16 h light/8 h dark.

Evolutionary Analysis of *CDC20.1* and *CDC20.2*

Sequence data used in this study were obtained from Phytozome 10.2 (http://phytozome.jgi.doe.gov/pz/portal.html). Synteny of CDC20 and

other genes in *A. thaliana*, *Arabidopsis lyrata*, *Capsella rubella*, *Brassica rapa*, and *Thellungiella halophila* was qualitatively determined using the Phytozome genome browser. Multiple sequences and protein amino acid sequences of all the duplicated gene pairs were aligned with ClustalW integrated in MEGA 5.2.2 (Tamura et al., 2011). The dS and dN (i.e., the number of synonymous and nonsynonymous substitutions per site) were determined using the aligned coding sequences by yn00 program in PAML 4.3 (Yang, 2007).

Accession Numbers

Sequence data from this article can be found in the Arabidopsis Genome Initiative database and the GenBank/EMBL libraries under the following accession numbers: *CDC20.1* (AT4G33270.1, NM_119482), *CDC20.2* (AT4G33260.1, NM_119480.3), *AUR1* (AT4G32830.1, NM_119436), and *EF1*α (AT5G65430, AK318784). The sequences used for evolutionary analysis in the following species can be found in the GenBank/EMBL libraries under the following accession numbers: *A. thaliana* (CDC20.1), NP_195053.1; *C. rubella* (CDC20.1), XP_006283703.1; *B. rapa* (CDC20.1), XP_009123591.1; *A. thaliana* (CDC20.2), NP_195052.1; *C. rubella* (CDC20.2), XP_006283731.1; and *B. rapa* (CDC20.2), XP_009138177.1. The *A. lyrata* CDC20.1 and CDC20.2 sequences are included in XP_002867190.1.

Supplemental Data

Supplemental Figure 1. Schematic Representation and Examination of *CDC20.1* Expression in Different Mutant Alleles.

Supplemental Figure 2. Mitosis Is Normal in *cdc20.1-3.*

Supplemental Figure 3. Localization of HTR12 in Wild Type and *cdc20.1*.

Supplemental Figure 4. *CDC20.2* Is Dispensable for Vegetative and Reproductive Development.

Supplemental Table 1. List of Primers Used in This Study.

ACKNOWLEDGMENTS

We thank Christopher Makaroff at Miami University for providing the SYN1 antibody, Pingli Lu for providing a vector with the *DMC1* promoter, and the ABRC at Ohio State University for providing the Arabidopsis mutant seeds. This work was supported by the Ministry of Science and Technology of China (2011CB944603), the National Natural Science Foundation of China (31370347 and 31570314), the International Technology Cooperation Project of Shanghai (13430720300), the Shanghai "Post-Qi-Ming-Xing Plan" for Young Scientists, China (13QA1400200), and by funds from Fudan University and Rijk Zwaan. G.P.C. was supported by a National Science Foundation grant (MCB-1121563).

AUTHOR CONTRIBUTIONS

B.N., Y.W., G.P.C., and H.M. designed the research. B.N. performed plant phenotypic observation, expression analysis, and plant transformation. L.W. performed statistic analysis of meiocyte distribution. B.N. and L.W. performed cytological experiments. D.R. constructed plasmids for plant transformation. L.Z. and R.R. did the phylogenetic analysis. B.N., L.W., and Y.W. analyzed the data. B.N., L.W., Y.W., G.C., and H.M. wrote the article.

Received October 1, 2015; revised November 16, 2015; accepted November 22, 2015; published December 15, 2015.

REFERENCES

Alonso, J.M., et al. (2003). Genome-wide insertional mutagenesis of *Arabidopsis thaliana.* Science **301:** 653–657.

Armstrong, S.J., Franklin, F.C.H., and Jones, G.H. (2003). A meiotic time-course for *Arabidopsis thaliana.* Sex. Plant Reprod. **16:** 141–149.

Cai, X., Dong, F., Edelmann, R.E., and Makaroff, C.A. (2003). The *Arabidopsis* SYN1 cohesin protein is required for sister chromatid arm cohesion and homologous chromosome pairing. J. Cell Sci. **116:** 2999–3007.

Caperta, A.D., Rosa, M., Delgado, M., Karimi, R., Demidov, D., Viegas, W., and Houben, A. (2008). Distribution patterns of phosphorylated Thr 3 and Thr 32 of histone H3 in plant mitosis and meiosis. Cytogenet. Genome Res. **122:** 73–79.

Castellano-Pozo, M., Santos-Pereira, J.M., Rondón, A.G., Barroso, S., Andújar, E., Pérez-Alegre, M., García-Muse, T., and Aguilera, A. (2013). R loops are linked to histone H3 S10 phosphorylation and chromatin condensation. Mol. Cell **52:** 583–590.

Chelysheva, L., Grandont, L., Vrielynck, N., le Guin, S., Mercier, R., and Grelon, M. (2010). An easy protocol for studying chromatin and recombination protein dynamics during *Arabidopsis thaliana* meiosis: immunodetection of cohesins, histones and MLH1. Cytogenet. Genome Res. **129:** 143–153.

Chu, T., Henrion, G., Haegeli, V., and Strickland, S. (2001). *Cortex*, a *Drosophila* gene required to complete oocyte meiosis, is a member of the Cdc20/fizzy protein family. Genesis **29:** 141–152.

Clough, S.J., and Bent, A.F. (1998). Floral dip: a simplified method for Agrobacterium-mediated transformation of *Arabidopsis thaliana.* Plant J. **16:** 735–743.

Cooper, K.F., and Strich, R. (2011). Meiotic control of the APC/C: similarities & differences from mitosis. Cell Div. **6:** 16.

Cooper, K.F., Mallory, M.J., Egeland, D.B., Jarnik, M., and Strich, R. (2000). Ama1p is a meiosis-specific regulator of the anaphase promoting complex/cyclosome in yeast. Proc. Natl. Acad. Sci. USA **97:** 14548–14553.

Cromer, L., Jolivet, S., Horlow, C., Chelysheva, L., Heyman, J., De Jaeger, G., Koncz, C., De Veylder, L., and Mercier, R. (2013). Centromeric cohesion is protected twice at meiosis, by SHUGOSHINs at anaphase I and by PATRONUS at interkinesis. Curr. Biol. **23:** 2090–2099.

Cromer, L., Heyman, J., Touati, S., Harashima, H., Araou, E., Girard, C., Horlow, C., Wassmann, K., Schnittger, A., De Veylder, L., and Mercier, R. (2012). OSD1 promotes meiotic progression via APC/C inhibition and forms a regulatory network with TDM and CYCA1;2/TAM. PLoS Genet. **8:** e1002865.

Dai, J., Sultan, S., Taylor, S.S., and Higgins, J.M. (2005). The kinase haspin is required for mitotic histone H3 Thr 3 phosphorylation and normal metaphase chromosome alignment. Genes Dev. **19:** 472–488.

Demidov, D., Lermontova, I., Weiss, O., Fuchs, J., Rutten, T., Kumke, K., Sharbel, T.F., Van Damme, D., De Storme, N., Geelen, D., and Houben, A. (2014). Altered expression of Aurora kinases in *Arabidopsis* results in aneu- and polyploidization. Plant J. **80:** 449–461.

Ditchfield, C., Johnson, V.L., Tighe, A., Ellston, R., Haworth, C., Johnson, T., Mortlock, A., Keen, N., and Taylor, S.S. (2003). Aurora B couples chromosome alignment with anaphase by targeting BubR1, Mad2, and Cenp-E to kinetochores. J. Cell Biol. **161:** 267–280.

Fang, G., Yu, H., and Kirschner, M.W. (1998). The checkpoint protein MAD2 and the mitotic regulator CDC20 form a ternary complex with the anaphase-promoting complex to control anaphase initiation. Genes Dev. **12:** 1871–1883.

Foley, E.A., and Kapoor, T.M. (2013). Microtubule attachment and spindle assembly checkpoint signalling at the kinetochore. Nat. Rev. Mol. Cell Biol. **14:** 25–37.

Gorbsky, G.J. (2015). The spindle checkpoint and chromosome segregation in meiosis. FEBS J. **282:** 2471–2487.

Hamant, O., Ma, H., and Cande, W.Z. (2006). Genetics of meiotic prophase I in plants. Annu. Rev. Plant Biol. **57:** 267–302.

Harms, E., Chu, T., Henrion, G., and Strickland, S. (2000). The only function of *Grauzone* required for *Drosophila* oocyte meiosis is transcriptional activation of the *cortex* gene. Genetics **155:** 1831–1839.

Hartwell, L.H., Mortimer, R.K., Culotti, J., and Culotti, M. (1973). Genetic control of the cell division cycle in yeast: V. genetic analysis of cdc mutants. Genetics **74:** 267–286.

Hauf, S., and Watanabe, Y. (2004). Kinetochore orientation in mitosis and meiosis. Cell **119:** 317–327.

Homer, H., Gui, L., and Carroll, J. (2009). A spindle assembly checkpoint protein functions in prophase I arrest and prometaphase progression. Science **326:** 991–994.

Houben, A., Demidov, D., Caperta, A.D., Karimi, R., Agueci, F., and Vlasenko, L. (2007). Phosphorylation of histone H3 in plants–a dynamic affair. Biochim. Biophys. Acta **1769:** 308–315.

Huang, C.H., et al. (2015) Resolution of Brassicaceae phylogeny using nuclear genes uncovers nested radiations and supports convergent morphological evolution. Mol. Biol. Evol., in press.

Izawa, D., and Pines, J. (2015). The mitotic checkpoint complex binds a second CDC20 to inhibit active APC/C. Nature **517:** 631–634.

Jiang, H., Wang, F.F., Wu, Y.T., Zhou, X., Huang, X.Y., Zhu, J., Gao, J.F., Dong, R.B., Cao, K.M., and Yang, Z.N. (2009). MULTIPOLAR SPINDLE 1 (MPS1), a novel coiled-coil protein of *Arabidopsis thaliana*, is required for meiotic spindle organization. Plant J. **59:** 1001–1010.

Jin, F., Hamada, M., Malureanu, L., Jeganathan, K.B., Zhou, W., Morbeck, D.E., and van Deursen, J.M. (2010). Cdc20 is critical for meiosis I and fertility of female mice. PLoS Genet. **6:** e1001147.

Kagale, S., Robinson, S.J., Nixon, J., Xiao, R., Huebert, T., Condie, J., Kessler, D., Clarke, W.E., Edger, P.P., Links, M.G., Sharpe, A.G., and Parkin, I.A. (2014). Polyploid evolution of the Brassicaceae during the Cenozoic era. Plant Cell **26:** 2777–2791.

Kang, J., and Yu, H. (2009). Kinase signaling in the spindle checkpoint. J. Biol. Chem. **284:** 15359–15363.

Kawabe, A., Matsunaga, S., Nakagawa, K., Kurihara, D., Yoneda, A., Hasezawa, S., Uchiyama, S., and Fukui, K. (2005). Characterization of plant Aurora kinases during mitosis. Plant Mol. Biol. **58:** 1–13.

Kawabe, A., Nasuda, S., and Charlesworth, D. (2006). Duplication of centromeric histone H3 (HTR12) gene in *Arabidopsis halleri* and *A. lyrata*, plant species with multiple centromeric satellite sequences. Genetics **174:** 2021–2032.

Kelly, A.E., Ghenoiu, C., Xue, J.Z., Zierhut, C., Kimura, H., and Funabiki, H. (2010). Survivin reads phosphorylated histone H3 threonine 3 to activate the mitotic kinase Aurora B. Science **330:** 235–239.

Kevei, Z., Baloban, M., Da Ines, O., Tiricz, H., Kroll, A., Regulski, K., Mergaert, P., and Kondorosi, E. (2011). Conserved CDC20 cell cycle functions are carried out by two of the five isoforms in *Arabidopsis thaliana.* PLoS One **6:** e20618.

Kim, J., et al. (2015). Meikin is a conserved regulator of meiosis-I-specific kinetochore function. Nature **517:** 466–471.

Kim, S., Meyer, R., Chuong, H., and Dawson, D.S. (2013). Dual mechanisms prevent premature chromosome segregation during meiosis. Genes Dev. **27:** 2139–2146.

Kudo, N.R., et al. (2006). Resolution of chiasmata in oocytes requires separase-mediated proteolysis. Cell **126:** 135–146.

Kurihara, D., Matsunaga, S., Omura, T., Higashiyama, T., and Fukui, K. (2011). Identification and characterization of plant Haspin kinase as a histone H3 threonine kinase. BMC Plant Biol. **11:** 73.

Mansfeld, J., Collin, P., Collins, M.O., Choudhary, J.S., and Pines, J. (2011). APC15 drives the turnover of MCC-CDC20 to make the spindle assembly checkpoint responsive to kinetochore attachment. Nat. Cell Biol. **13:** 1234–1243.

Manzanero, S., Arana, P., Puertas, M.J., and Houben, A. (2000). The chromosomal distribution of phosphorylated histone H3 differs between plants and animals at meiosis. Chromosoma **109:** 308–317.

Morrow, C.J., Tighe, A., Johnson, V.L., Scott, M.I., Ditchfield, C., and Taylor, S.S. (2005). Bub1 and aurora B cooperate to maintain BubR1-mediated inhibition of APC/C^{Cdc20}. J. Cell Sci. **118:** 3639–3652.

Musacchio, A., and Ciliberto, A. (2012). The spindle-assembly checkpoint and the beauty of self-destruction. Nat. Struct. Mol. Biol. **19:** 1059–1061.

Nagaoka, S.I., Hodges, C.A., Albertini, D.F., and Hunt, P.A. (2011). Oocyte-specific differences in cell-cycle control create an innate susceptibility to meiotic errors. Curr. Biol. **21:** 651–657.

Oelschlaegel, T., Schwickart, M., Matos, J., Bogdanova, A., Camasses, A., Havlis, J., Shevchenko, A., and Zachariae, W. (2005). The yeast APC/C subunit Mnd2 prevents premature sister chromatid separation triggered by the meiosis-specific APC/C-Ama1. Cell **120:** 773–788.

Page, A.W., and Orr-Weaver, T.L. (1996). The *Drosophila* genes *grauzone* and *cortex* are necessary for proper female meiosis. J. Cell Sci. **109:** 1707–1715.

Paula, C.M., Techio, V.H., Sobrinho, F.S., and Freitas, A.S. (2013). Distribution pattern of histone H3 phosphorylation at serine 10 during mitosis and meiosis in *Brachiaria* species. J. Genet. **92:** 259–266.

Pesin, J.A., and Orr-Weaver, T.L. (2008). Regulation of APC/C activators in mitosis and meiosis. Annu. Rev. Cell Dev. Biol. **24:** 475–499.

Peters, J.M. (2006). The anaphase promoting complex/cyclosome: a machine designed to destroy. Nat. Rev. Mol. Cell Biol. **7:** 644–656.

Peterson, R., Slovin, J.P., and Chen, C. (2010). A simplified method for differential staining of aborted and non-aborted pollen grains. J. Integr. Plant Biol. **1:** 13.

Riedel, C.G., et al. (2006). Protein phosphatase 2A protects centromeric sister chromatid cohesion during meiosis I. Nature **441:** 53–61.

Riehs, N., Akimcheva, S., Puizina, J., Bulankova, P., Idol, R.A., Siroky, J., Schleiffer, A., Schweizer, D., Shippen, D.E., and Riha, K. (2008). *Arabidopsis* SMG7 protein is required for exit from meiosis. J. Cell Sci. **121:** 2208–2216.

Sacristan, C., and Kops, G.J. (2015). Joined at the hip: kinetochores, microtubules, and spindle assembly checkpoint signaling. Trends Cell Biol. **25:** 21–28.

Salah, S.M., and Nasmyth, K. (2000). Destruction of the securin Pds1p occurs at the onset of anaphase during both meiotic divisions in yeast. Chromosoma **109:** 27–34.

Saurin, A.T., van der Waal, M.S., Medema, R.H., Lens, S.M., and Kops, G.J. (2011). Aurora B potentiates Mps1 activation to ensure rapid checkpoint establishment at the onset of mitosis. Nat. Commun. **2:** 316.

Singh, S.A., Winter, D., Kirchner, M., Chauhan, R., Ahmed, S., Ozlu, N., Tzur, A., Steen, J.A., and Steen, H. (2014). Co-regulation proteomics reveals substrates and mechanisms of APC/C-dependent degradation. EMBO J. **33:** 385–399.

Smith, T.F., Gaitatzes, C., Saxena, K., and Neer, E.J. (1999). The WD repeat: a common architecture for diverse functions. Trends Biochem. Sci. **24:** 181–185.

Sudakin, V., Chan, G.K., and Yen, T.J. (2001). Checkpoint inhibition of the APC/C in HeLa cells is mediated by a complex of BUBR1, BUB3, CDC20, and MAD2. J. Cell Biol. **154:** 925–936.

Sun, S.C., and Kim, N.H. (2012). Spindle assembly checkpoint and its regulators in meiosis. Hum. Reprod. Update **18:** 60–72.

Swan, A., and Schüpbach, T. (2007). The Cdc20 (Fzy)/Cdh1-related protein, Cort, cooperates with Fzy in cyclin destruction and anaphase progression in meiosis I and II in *Drosophila.* Development **134:** 891–899.

Talbert, P.B., Masuelli, R., Tyagi, A.P., Comai, L., and Henikoff, S. (2002). Centromeric localization and adaptive evolution of an *Arabidopsis* histone H3 variant. Plant Cell **14:** 1053–1066.

Tamura, K., Peterson, D., Peterson, N., Stecher, G., Nei, M., and Kumar, S. (2011). MEGA5: molecular evolutionary genetics analysis using maximum likelihood, evolutionary distance, and maximum parsimony methods. Mol. Biol. Evol. **28:** 2731–2739.

Tan, G.S., Magurno, J., and Cooper, K.F. (2011). Ama1p-activated anaphase-promoting complex regulates the destruction of Cdc20p during meiosis II. Mol. Biol. Cell **22:** 315–326.

Teixeira, J.H., Silva, P.M., Reis, R.M., Moura, I.M., Marques, S., Fonseca, J., Monteiro, L.S., and Bousbaa, H. (2014). An overview of the spindle assembly checkpoint status in oral cancer. BioMed Res. Int. **2014:** 145289.

Terret, M.E., Wassmann, K., Waizenegger, I., Maro, B., Peters, J.M., and Verlhac, M.H. (2003). The meiosis I-to-meiosis II transition in mouse oocytes requires separase activity. Curr. Biol. **13:** 1797–1802.

Uhlmann, F. (2001). Chromosome cohesion and segregation in mitosis and meiosis. Curr. Opin. Cell Biol. **13:** 754–761.

Van Damme, D., De Rybel, B., Gudesblat, G., Demidov, D., Grunewald, W., De Smet, I., Houben, A., Beeckman, T., and Russinova, E. (2011). *Arabidopsis* α Aurora kinases function in formative cell division plane orientation. Plant Cell **23:** 4013–4024.

Wang, F., Dai, J., Daum, J.R., Niedzialkowska, E., Banerjee, B., Stukenberg, P.T., Gorbsky, G.J., and Higgins, J.M.G. (2010). Histone H3 Thr-3 phosphorylation by Haspin positions Aurora B at centromeres in mitosis. Science **330:** 231–235.

Wang, F., Ulyanova, N.P., Daum, J.R., Patnaik, D., Kateneva, A.V., Gorbsky, G.J., and Higgins, J.M. (2012). Haspin inhibitors reveal centromeric functions of Aurora B in chromosome segregation. J. Cell Biol. **199:** 251–268.

Wang, M., Tang, D., Luo, Q., Jin, Y., Shen, Y., Wang, K., and Cheng, Z. (2012). BRK1, a Bub1-related kinase, is essential for generating proper tension between homologous kinetochores at metaphase I of rice meiosis. Plant Cell **24:** 4961–4973.

Wang, Y., Cheng, Z., Huang, J., Shi, Q., Hong, Y., Copenhaver, G.P., Gong, Z., and Ma, H. (2012). The DNA replication factor RFC1 is required for interference-sensitive meiotic crossovers in *Arabidopsis thaliana.* PLoS Genet. **8:** e1003039.

Wang, Y., Cheng, Z., Lu, P., Timofejeva, L., and Ma, H. (2014). Molecular cell biology of male meiotic chromosomes and isolation of male meiocytes in *Arabidopsis thaliana.* Methods Mol. Biol. **1110:** 217–230.

Wang, Y., Magnard, J.L., McCormick, S., and Yang, M. (2004). Progression through meiosis I and meiosis II in *Arabidopsis* anthers is regulated by an A-type cyclin predominately expressed in prophase I. Plant Physiol. **136:** 4127–4135.

Wassmann, K., Niault, T., and Maro, B. (2003). Metaphase I arrest upon activation of the Mad2-dependent spindle checkpoint in mouse oocytes. Curr. Biol. **13:** 1596–1608.

Watanabe, Y. (2012). Geometry and force behind kinetochore orientation: lessons from meiosis. Nat. Rev. Mol. Cell Biol. **13:** 370–382.

Whitfield, Z.J., Chisholm, J., Hawley, R.S., and Orr-Weaver, T.L. (2013). A meiosis-specific form of the APC/C promotes the oocyte-to-embryo transition by decreasing levels of the Polo kinase inhibitor matrimony. PLoS Biol. **11:** e1001648.

Yamagishi, Y., Honda, T., Tanno, Y., and Watanabe, Y. (2010). Two histone marks establish the inner centromere and chromosome bi-orientation. Science **330:** 239–243.

Yang, H., Lu, P., Wang, Y., and Ma, H. (2011). The transcriptome landscape of *Arabidopsis* male meiocytes from high-throughput sequencing: the complexity and evolution of the meiotic process. Plant J. **65:** 503–516.

Yang, W.L., Li, J., An, P., and Lei, A.M. (2014). CDC20 down-regulation impairs spindle morphology and causes reduced first polar body emission during bovine oocyte maturation. Theriogenology **81:** 535–544.

Yang, Z. (2007). PAML 4: phylogenetic analysis by maximum likelihood. Mol. Biol. Evol. **24:** 1586–1591.

Zamariola, L., De Storme, N., Tiang, C.L., Armstrong, S.J., Franklin, F.C.H., and Geelen, D. (2013). *SGO1* but not *SGO2* is required for maintenance of centromere cohesion in *Arabidopsis thaliana* meiosis. Plant Reprod. **26:** 197–208.

Zamariola, L., Tiang, C.L., De Storme, N., Pawlowski, W., and Geelen, D. (2014). Chromosome segregation in plant meiosis. Front. Plant Sci. **5: 279.**

Zich, J., and Hardwick, K.G. (2010). Getting down to the phosphorylated 'nuts and bolts' of spindle checkpoint signalling. Trends Biochem. Sci. **35:** 18–27.

Supplemental Figures and Table

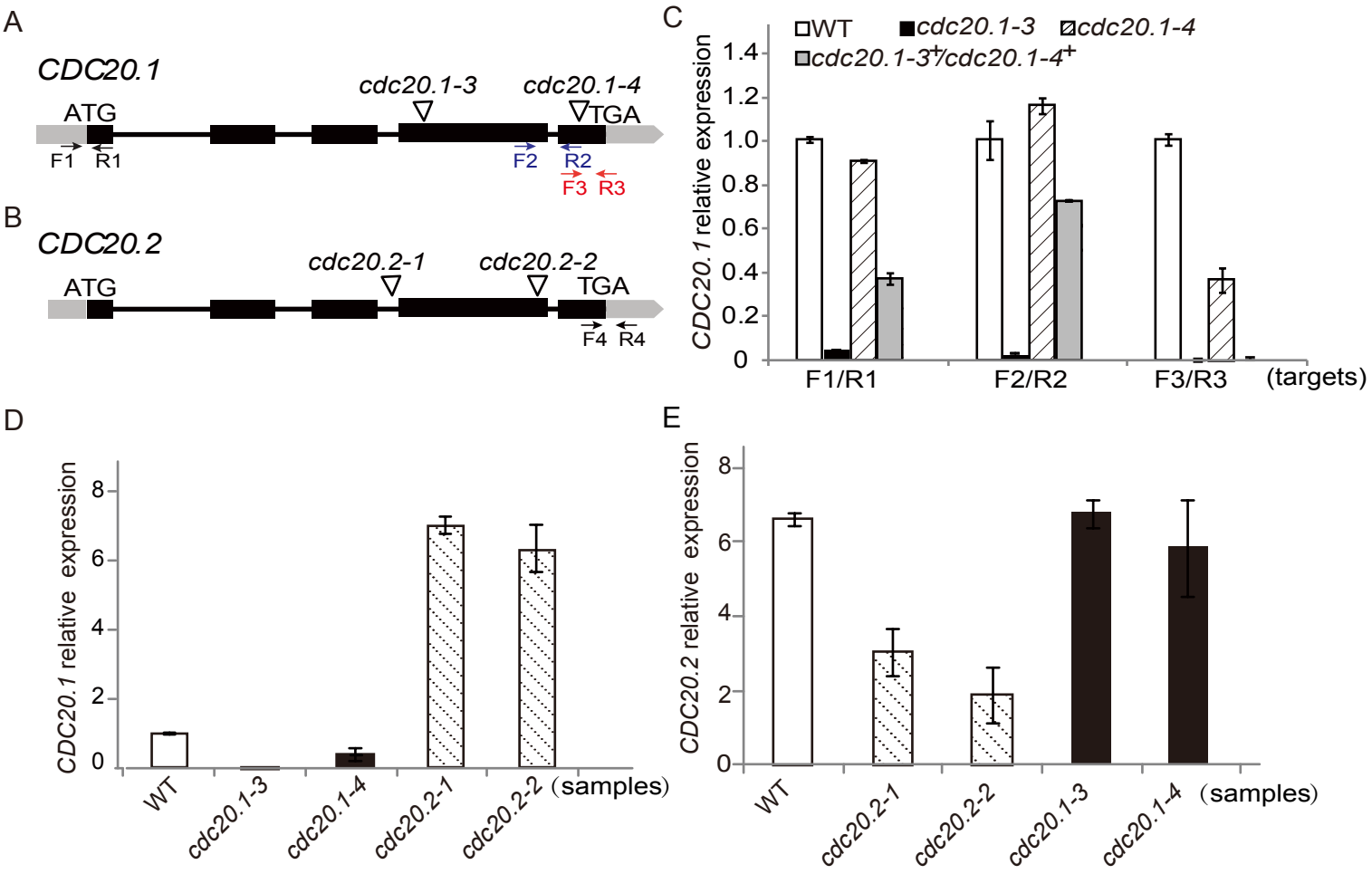

Supplemental Figure 1. Schematic Representation and Examination of *CDC20.1* Expression in Different Mutant Alleles.

(A) Schematic representation of Arabidopsis *CDC20.1* with T-DNA insertions (inverted triangles) in *cdc20.1-3* and *cdc20.1-4*. The positions of the primers used for RT-qPCR are indicated.

(B) Schematic representation of *CDC20.2* with T-DNA insertions in *cdc20.2-1* and *cdc20.2-2* alleles. Exons are shown as boxes (gray: UTR, black: CDS); and arrows indicate primer positions.

(C) Real-time PCR amplification of the truncated transcripts from *CDC20.1* loci in T-DNA insertional mutant alleles using different primers as shown in **(A)**.

(D) Real-time PCR amplification of *CDC20.1* in WT and T-DNA insertion mutant alleles of *cdc20.1-3, cdc20.1-4, cdc20.2-1* and *cdc20.2-2* using primers F3/R3 indicated in **(A)**.

(E) Real-time PCR amplification of of *CDC20.2* in WT and T-DNA insertional mutant alleles of *cdc20.2-1, cdc20.2-2, cdc20.1-3 and cdc20.1-4* using primers F4/R4 as shown in **(B)**.

EF1α was used as the internal control **(C-E)**. The experiment was conducted in three technical replicates and error bars indicate SD.

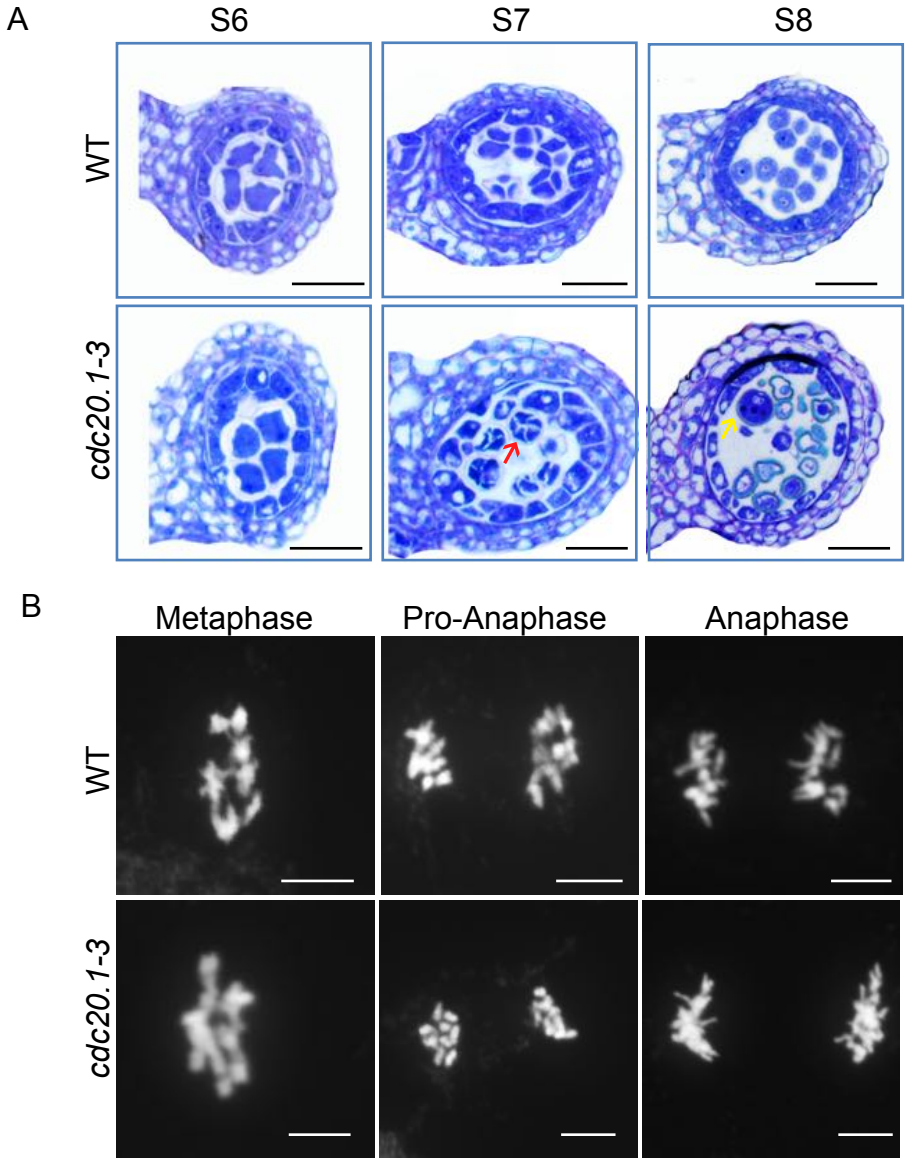

Supplemental Figure 2. Mitosis is Normal in *cdc20.1-3.*

(A) Semi-thin section of anthers at stage 6 (S6), stage 7 (S7) and stage 8 (S8) in WT (top) and *cdc20.1-3* (bottom). The *cdc20.1-3* anthers form polyads (red arrow) with more than four microspores and different sizes of pollen grain (yellow arrow). Bars=10 μm.

(B) Mitotic chromosome phenotypes in WT (top) and *cdc20.1-3* (bottom). Bars=5 μm.

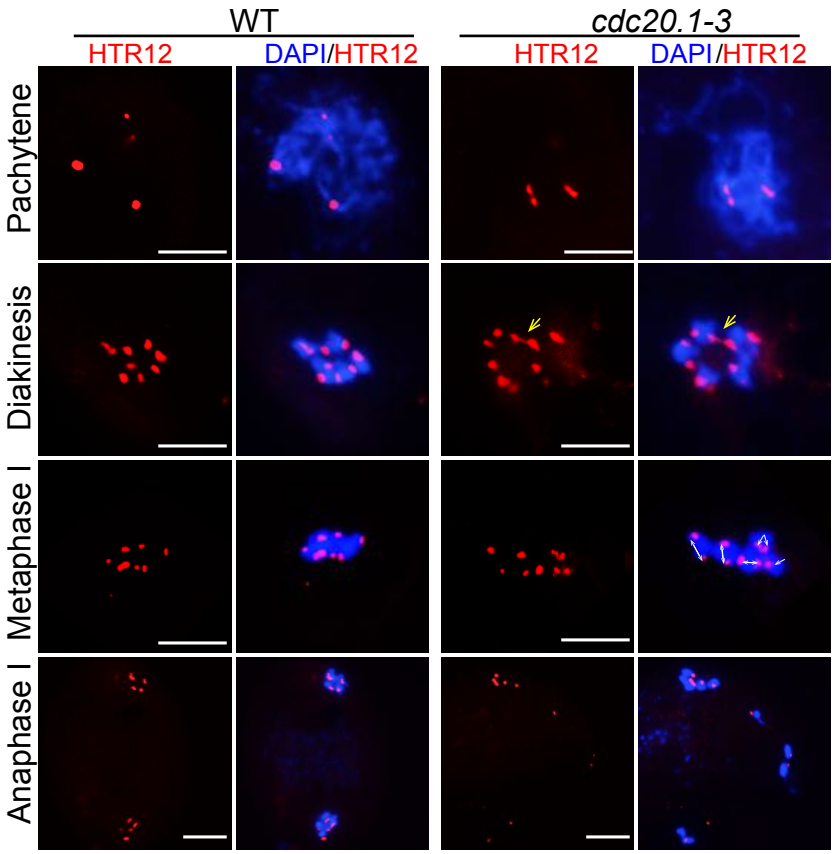

Supplemental Figure 3. Localization of HTR12 in WT and *cdc20.1-3*. Immunolocalization of HTR12 (red) on DAPI stained chromosomes (blue) of WT and *cdc20.1-3* at diakinesis, metaphase I and Anaphase I Bivalents in *cdc20.1-3* associate at diakinesis (yellow arrows) and misorient (white double arrows) at metaphase I. Bars=5 μm.

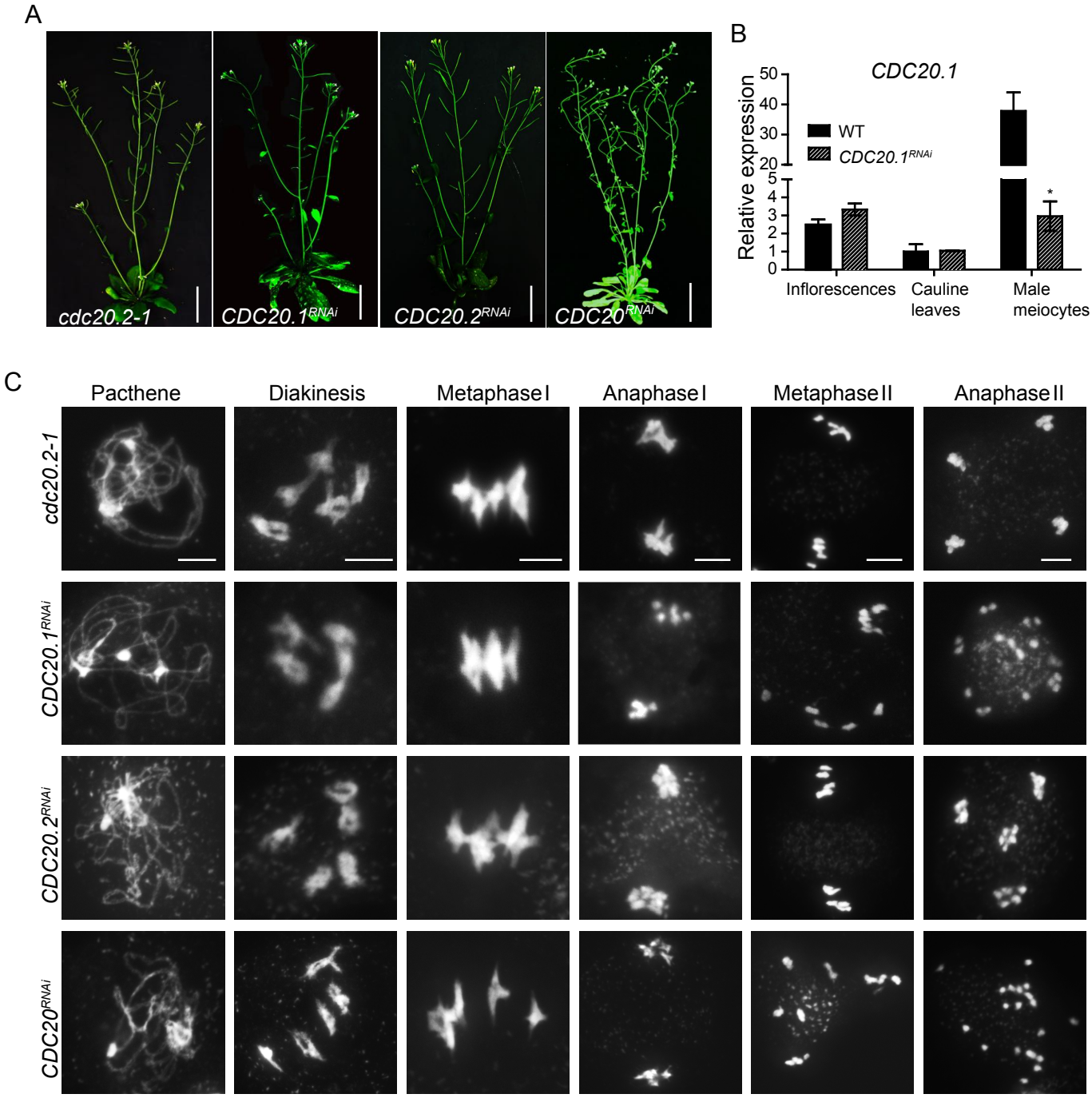

Supplemental Figure 4. *CDC20.2* is Dispensable for Vegetative and Reproductive Development.

(A) Phenotypes of *cdc20.2-1*, *ProDMC1:CDC20.1*^{RNAi}, *ProDMC1:CDC20.1*^{RNAi} and *ProDMC1:CDC20*^{RNAi} transgenic plant. Bars=5 cm.

(B) Expression of *CDC20.1* in WT and *ProDMC1:CDC20.1*^{RNAi}.

(C) Meiotic chromosome phenotypes of *cdc20.2-1*, *ProDMC1:CDC20.1*^{RNAi}, *ProDMC1:CDC20.2*^{RNAi} and *ProDMC1:CDC20*^{RNAi} at different stages. Bars=5 μm.

Supplemental Table 1. List of Primers Used in This Study

Purpose	**Primer name**	**Primer sequence (5' to 3')**
CDC20.1.3 Genotyping	CS369798F	GATTTAGTTGTTTTCCTTTACC
	CS369798R	CTGAAGTCCAGCTGTGGGAT
	pAC161	GGGCTACACTGAATTGGT
CDC20.1.4 Genotyping	CS369975F	ATGCAAGCAAATAAGTTTGACT
	CS369975R	GGTAAAGGAAAACAACTAAATC
	PADIS1	GGGCTACACTGAATTGGT
CDC20.2.1 Genotyping	SALK_136710F	TGAATGACCTCAAAGACTCA
	SALK_136710R	GATGTGTTTCTCATATTTCT
	SALK -LBb1.3	ATTTTGCCGATTTCGGAAC
CDC20.2.2 Genotyping	SALK_114279F	AGAAATATGAGAAACACATC
	SALK_114279R	GACCCATATCATTGATGAATC
	SALK -LBb1.3	ATTTTGCCGATTTCGGAAC
qRT-PCR (*CDC20.1*)	CDC20.1F1	ACCCAATCTACTCTCGATTC
	CDC20.1R1	AGCCTGCGTCTTGTAGTGAG
	CDC20.1F2	CGGGTTTACACAGAATCAGCTC
	CDC20.1R2	ATTCCAGAACCTCAGAGTCTCA
	CDC20.1F3	TGAGACTCTGAGGTTCTGGAAT
	CDC20.1R3	GCAAATAAGTTTGACTCA
qRT-PCR (*CDC20.2*)	CDC20.2F4	TGAGACTCTGAGGTTCTGGAAT
	CDC20.2R4	GCAAATAAGTTTGACTCA
qRT-PCR (*EF1α*)	EF1α-F	GGTGGTATTGACAAGCGTG
	EF1α-R	GATTTCATCGTACCTAGCC
DMC1::CDC20.1 -RNAi	CDC20.1(*Nco* I)1st- F	CA**TGCCAT**ACCCAATCTACTCTCGAT TC
	CDC20.1(*Spe* I)1st-R	GG**ACTAGT**AGCCTGCGTCTTGTAGT GAG
	CDC20.1(*Xba* I)2nd-F	GG**TCTAGA**ACCCAATCTACTCTCGA TTC
	CDC20.1(*Sal* I)2nd-R	GCG**TCGACA**GCCTGCGTCTTGTAGT GAG
DMC1::CDC20.2 -RNAi	CDC20.2(*Nco* II)1st-F	CATG**CCATGG**CATGATTGGCTCTACCCCTTTA TAAG
	CDC20.2(*Spe* I)1st-R	GG**ACTAGT**CCCACCGATTCAAACCTGCATC
	CDC20.2(*Sal* I)2nd-F	ACGC**GTCGAC**GTATTGGCTCTACCCC TTTATAAG
	CDC20.2-(*Xba* I)2nd-R	GC**TCTAGA**GCCACCGATTCAAACCT GCATC
DMC1 ::-*CDC20* -RNAi	CDC20- (*Spe* I-*Sal* I)-F	ACGC**ACTAGT**GG**GTCGAC**GATCAGA TCACCCATTGTGGA
	CDC20-(NcoI-XbaI)-R	GC**CCATGG**GC**TCTAGA**AACTCTCTTTCATTCT TGCTC
DMC1::AUR1 -RNAi	AUR1II(*Nco* II)1st-F	TGGA**CCATGG**ATGGCGATCCCTACGGAGAC
	AUR1-(*Spe* I)1st-R	G**ACTAGT**GTAGCAGCTCGTCTTTCGCTGA
	AUR1-(*Xba* I)2nd-F	GC**TCTAGA**ATGGCGATCCCTACGGA GAC
	AUR1-((*Sal* I)2nd-R	ACGC**GTCGA**CGTAGCAGCTCGTCTTT
qRT-PCR (*AUR1*)	AUR1-F	CACCAATTGGATTTGGATCT
	AUR1-R	GATAGACGTGACCGAATTTGC